Research Square

Preprints are preliminary reports that have not undergone peer review. They should not be considered conclusive, used to inform clinical practice, or referenced by the media as validated information.

A Critical Role for The COP9 Signalosome Subunit 3 as A Gatekeeper of Genome Integrity in 2-Cell Mouse Embryos

Steffen Israel
Max Planck Institute for Molecular Biomedicine
Hannes Drexler
Max Planck Institute for Molecular Biomedicine
Georg Fuellen
Rostock University Medical Center, Institute for Biostatistics and Informatics in Medicine and Aging Research
Michele Boiani (mboiani@mpi-muenster.mpg.de)
Max Planck Institute for Molecular Biomedicine

Research Article

Keywords: COP9 signal transduction complex (signalosome), totipotency, 2-cell blastomere, proteome, TRipartite Motif containing-21 (TRIM21), mouse, COPS3

Posted Date: January 4th, 2021

DOI: https://doi.org/10.21203/rs.3.rs-135716/v1

License: This work is licensed under a Creative Commons Attribution 4.0 International License.
Read Full License

A critical role for the COP9 signalosome subunit 3 as a gatekeeper of genome integrity in 2-cell mouse embryos

Steffen Israel [1], Hannes C.A. Drexler [1], Georg Fuellen [2] and Michele Boiani [1,*]
[1] Max Planck Institute for Molecular Biomedicine, Roentgenstrasse 20, 48149 Muenster, Germany
[2] Rostock University Medical Center, Institute for Biostatistics and Informatics in Medicine and Aging Research (IBIMA), Ernst-Heydemann-Strasse 8, 18057 Rostock, Germany
*: corresponding author, Email address: mboiani@mpi-muenster.mpg.de

Abstract

Investigations of genes required in early mammalian development are complicated by protein deposits of maternal products, which continue to operate after the gene locus has been disrupted. This leads to an underestimation of the number of genes known to be needed during the embryonic phase of cellular totipotency (up to the 4-cell stage). Here, we expose a critical role of the gene *Cops3* by showing that it protects genome integrity during the 2-cell stage of mouse embryo development, in contrast to the previous functional assignment at postimplantation. This new role is mediated by a large, stable and hitherto overlooked deposit of maternal protein. Since protein abundance and stability defeat prospects of DNA- or RNA-based gene inactivation, we adopted a protein strategy of gene inactivation: antigen masking or TRIM21-mediated proteasomal degradation of COPS3. Both resulted in 2-cell embryo lethality, but the expected degradation remained outstanding, because the major fraction of the total COPS3 is secluded in a submembrane cortical rim that withstands extraction with detergent, thereby exposing a soluble vs. insoluble fraction of COPS3, which we ascribe with distinct functional properties. In mechanistic terms, transcriptomic and metabolic analyses reveal that soluble COPS3 is involved in several processes, which, however, converge on DNA endoreduplication and the accumulation of DNA strand breaks in the 2-cell nucleus, where the minor soluble fraction of COPS3 is placed. Thus, we have shown the critical role of maternal protein deposits in development, and we have also highlighted the distinction between the site of accumulation (cell cortex) and point of use (nucleus), which is a dimension of the protein-based strategies of gene inactivation not yet fully appreciated.

Word count: 269

Large scale data are available via Gene Expression Omnibus with the identifier GSE155205, and ProteomeXchange with the identifier PXD017212.

Keywords: COP9 signal transduction complex (signalosome), totipotency, 2-cell blastomere, proteome, TRipartite Motif containing-21 (TRIM21), mouse, COPS3

Introduction

Genes critical for the earliest stages of development have been known for a long time. Mouse embryos with mutations in these genes typically die during or shortly after the blastocyst stage, i.e. after the phase of cellular totipotency, which is over by the 4-cell stage as measured by the ability of isolated blastomeres to build viable blastocysts comprised of trophectoderm, primitive endoderm and epiblast [1,2]. The number of genes shown experimentally to be required prior to the blastocyst stage is relatively small. Exemplarily, of 712 candidate genes screened in a large-scale functional study using RNA interference, only 4 gene interferences resulted in cleavage stage embryo arrest and 20 interferences prevented blastocyst formation [3]. Of 347 genes whose gene ontology (GO) annotations matched the major DNA repair pathways according to the Mouse Genome Informatics Gene Ontology Project (MGI-GO) database, only 10 genes had a lethal knockout phenotype which manifests itself during the totipotent phase or by the blastocyst stage [4]. These small numbers are probably underestimated, due to an earlier accumulation of downstream product (transcript or protein), prior to experimental mutagenesis. This means that the first time point when a given gene is required for embryogenesis (the "first-time requirement") may have been overlooked in some cases, and the severity of developmental consequences is higher when this time point concerns the totipotent blastomeres.

We noted previously that the peri-zygotic transcriptional dynamics of the gene *Cops3* (i.e. non-homogeneous mRNA distribution in the oocyte and difference of mRNA level between 2-cell blastomeres [5]) is not consistent with a first-time requirement of this gene at postimplantation, as inferred from the timing of death of *Cops3* knock-out embryos [6]. Furthermore, the observed *in situ* distribution of the *Cops3* mRNA [5] is reminiscent of developmental mosaicism, which is a controversial issue in mammals [7]. *Cops3* encodes a subunit of the Constitutive Photomorphogenic 9 (COP9) signalosome complex, whose subunits operate together (as a holocomplex) or as monomers [8], as regulators of a wide range of biological processes that are ubiquitous in cells of plants and animals. Protein degradation is the process most studied, but COPS3 is also a transcriptional regulator, and a player in DNA repair and other functions [9-14]. In contrast to this variety of roles in the soma, the roles of COP9 or its subunits are still poorly characterized in the mammalian germline. Current knowledge points at germline stem cell survival [15,16], meiosis [17] and epiblast survival in the postimplantation embryo [6], while the preimplantation embryo seems unaffected. We were, therefore, surprised to find that when 2-cell mouse embryos were bisected and followed up in development, the *Cops3* mRNA inter-blastomere difference correlated, three

days later, with the number of epiblast cells found in monozygotic twin blastocysts derived from the sister blastomeres [5,18,19].

In the present study, we bring to light a critical role for *Cops3* during the initial and totipotent phase of mouse embryo development. When a gene product accumulates in oocytes, and even more so if the protein is abundant and stable, it becomes difficult to generate loss of function phenotypes using standard genetic knockout or RNA knockdown techniques. Therefore we harnessed two protein-based strategies to inactivate the COPS3 protein directly instead of its encoding transcript: 1) The antigen masking method, in which the protein of interest is prevented from performing its function [20], and 2) the TRIM21-proteasomal method, in which the E3 ubiquitin-protein ligase TRIM21 (TRIpartite Motif containing-21, also known as Ro52) ubiquitinates and commits the protein of interest for degradation – hence the nickname 'Trim-away' [21]. Our COPS3 results reveal how the inactivation of a gene product on the protein level can expose a phenotype very different from that of genetic techniques and suggest that assigning genes to roles in embryogenesis may be less safe than assumed, if the protein products of these genes accumulate in oocytes. Moreover, we demonstrate that aspects of subcellular localization must be carefully considered in the design of a 'Trim-away' experiment, and in the interpretation of its results.

Results

Cops3 forms a large protein deposit, divided between a cortical and a nuclear pool, in mouse oocytes and embryos

As we scrutinized the expression of *Cops3* during preimplantation mouse embryo development we realized that the bulk of gene product was supplied by the oocyte to the embryo as a protein (Figure 1A), as measured by liquid chromatography-mass spectrometry (LC-MS/MS) using the 'relative Intensity Based Absolute Quantification' (riBAQ) algorithm [22-25]. COPS3 abundance was high, in the range of the maternal-effect genes (Figure 1A), and decreased from oocyte to blastocyst, in contrast to *Cops3* mRNA (Figure 1B). We identified two monoclonal antibodies, a rabbit (RabMab®) and a mouse one, both of which recognized a single band of the correct molecular weight in Western blots of cell lysates (Figure 1C; the full-length blots are presented in Supplementary Figure 1). Immunofluorescence analysis revealed a cortical rim of COPS3 underneath the cell membrane, excluded from regions of cell-cell contact and from the polar body, during the first half of preimplantation development. Subsequently this cortical localization was replaced by a nuclear localization during the second half of preimplantation development (Figure 1D). A cortical rim was also seen for another subunit of the same complex as COPS3, namely COPS5 (Supplementary Figure 2), thereby supporting the authenticity of the rim structure.

Clearly, in a case like this, trying to remove the COPS3 protein in oocytes by acting on its precursor mRNA may not result in the depletion expected. Therefore, there is scope for proposing that 1) the protein may support the biological functions associated with *Cops3* even before the gene is transcriptionally upregulated, and that 2) investigations into the consequences of protein depletion should be conducted by targeting the protein COPS3 directly and not its precursor mRNA.

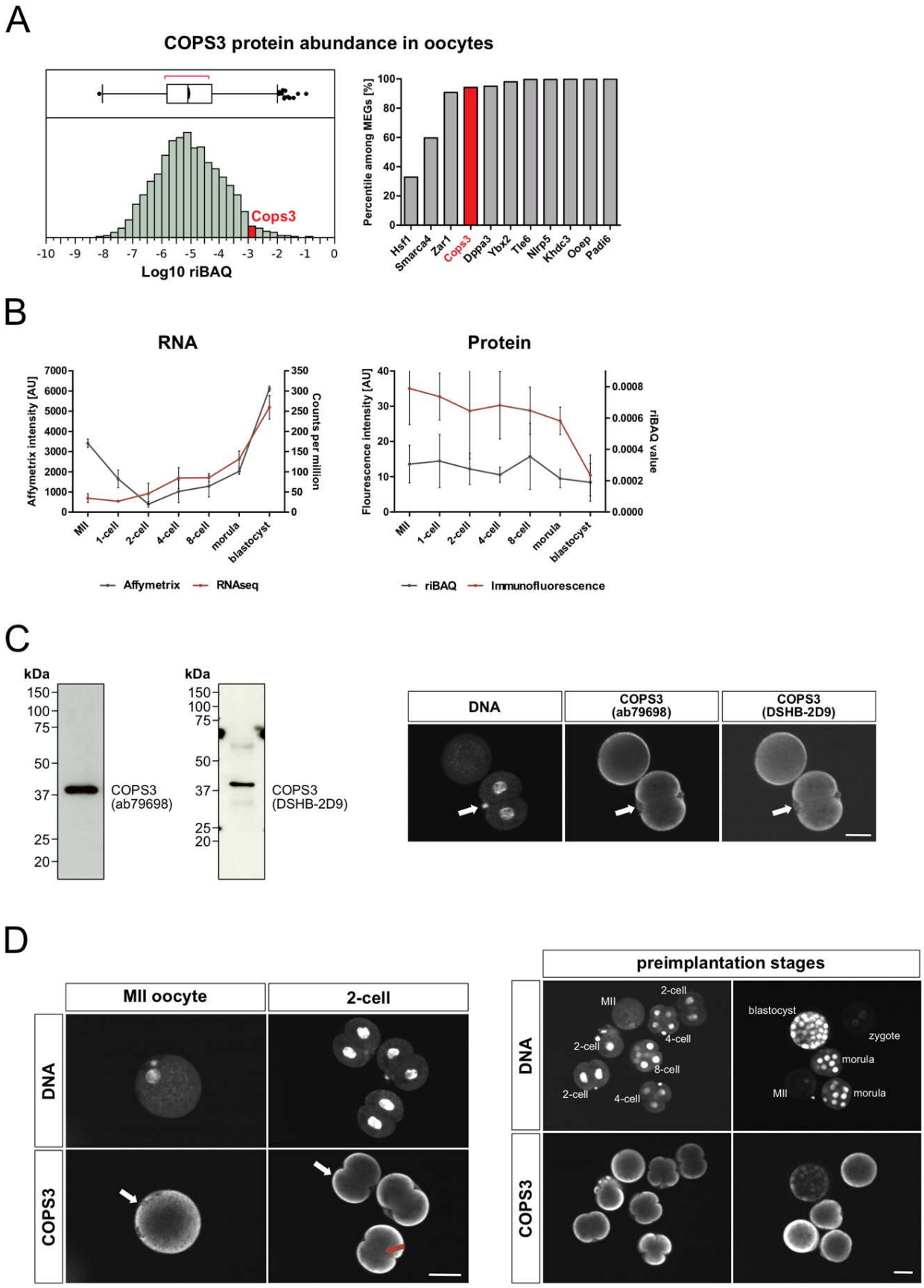

Figure 1. Protein and transcript expression of *Cops3* in mouse preimplantation development. (A). Left: Genome-wide distribution of protein abundances (riBAQ) in oocytes. Right: Compared to maternal factors known to be accumulated in oocytes, the abundance of COPS3 ranks high in the 94th percentile. **(B).** Abundance profile of *Cops3* mRNA and

COPS3 protein, each measured by two independent methods; data are presented as means and standard deviations (for RNA, 100 oocytes or embryos per stage in two replicates; for protein, 200-600 oocytes or embryos per stage in three proteomic replicates, and at least 3 oocytes or embryos per stage for immunofluorescence; transcriptome/proteome datasets are extracted from [26] and are provided here in Supplementary Tables 1 and 2). **(C).** Specificity of the two monoclonal antibodies against COPS3 used in this study, RabMab® (ab79698) and mouse (DSHB-2D9), as documented by the single band in Western blot (lysate of MEFs or ES cells) and by the subcellular distribution within the same 2-cell embryos after immunofluorescence with both antibodies. The full-length blots are presented in Supplementary Figure 1. White arrow points at the non-stained polar body next to the positive rim. Note the lower background, i.e. the better signal-to-noise ratio, of the RabMab®. DNA was stained with YO-PRO-1. **(D).** Left: Developmental localization of COPS3 in oocyte and 2-cell stage, visualized by the RabMab® antibody, with white arrows pointing at the cortical rim and red arrow pointing at the signal exclusion from regions of cell-cell contact. Right: Developmental localization of COPS3 in preimplantation stages; note the prominence of the cortical rim up to the 4-cell stage, starting to fade thereafter, and being replaced by a nuclear signal distribution at the blastocyst stage. DNA was stained with YO-PRO-1. Abbreviations: Affymetrix stands for microarray; AU, arbitrary units; ES cells, embryonic stem cells; MEFs, mouse embryonic fibroblasts; MEG, maternal-effect genes; kDa, kiloDalton. riBAQ, relative intensity-based absolute quantification. Size bar: 50 µm.

Progression through second embryonic cell cycle is severely hampered by inhibition of maternal COPS3

We adopted a dual strategy of protein inactivation, in contrast to the conventional but indirect way of interfering with the mRNA precursor or the DNA template, to ascertain the need for *Cops3* during the initial phase of mouse embryo development. We operated this inactivation either before or after the stimulus that triggers development. For practical reasons, we started out with oocytes which had already received the stimulus of fertilization (zygotes), since they are more tolerant of the large microinjection volumes used in our protocol [22] compared to pre-stimulus (MII) oocytes. We microinjected zygotes with defined amounts of either of the two anti-COPS3 monoclonal antibodies (Figure 1C), in highly purified form (see Methods), to match the amount of COPS3 present in the cell, as known from our published proteomic catalogue [22]. Fluorescence of the co-microinjected inert tracer (Oregon-Green dextran beads: OGDB) confirmed that the microinjections had been successful in all cases. Most of the microinjected zygotes arrested at the 2-cell stage (Figure 2A), which was due to the antibody, since microinjection of wt zygotes with the sole antibody buffer supported blastocyst formation, as did an antibody against GFP protein, which is not present in wt cells (Figure 2C). These results document that COPS3 is needed earlier in development than thought previously [6]. Since this earlier phenotype precedes the transcriptional upregulation of *Cops3* during embryo cleavage (Figure 1B), it also means that the earlier phenotype hinges on the maternal protein.

Albeit impeded in its functional interactions, COPS3 had only been bound but not degraded by the antibodies. Therefore, we also employed a degradation of the COPS3 antibody complex, via

TRIM21-mediated proteasomal degradation. This was achieved by overexpression of TRIM21, imposed via microinjection of *mCherry-TRIM21* mRNA, thereby triggering the proteasomal commitment of the ternary complex formed between target protein, the co-injected COPS3 antibody and TRIM21 [21]. Throughout the text, *Trim21* mRNA and TRIM21 protein are always intended as tagged with *mCherry* sequence and mCHERRY peptide, respectively. Zygotes microinjected with COPS3 RabMab® antibody and *mCherry-TRIM21* mRNA arrested at the 2-cell stage, with a negligible number of embryos that made it beyond (Figure 2B), in contrast to efficient blastocyst progression of zygotes injected with the buffer of anti-COPS3 or an anti-GFP antibody (Figure 2C). These observations were mirrored in zygotes microinjected with the mouse monoclonal antibody. In addition, and irrespective of which of the two antibodies was used, the 2-cell arrest also occurred when COPS3 inactivation was operated prior to the developmental stimulus. To this end, MII oocytes were microinjected with COPS3 antibody and *mCherry-TRIM21* mRNA and then subjected to parthenogenetic activation. The majority of the parthenogenetic embryos (N = 43) were arrested at the 1-cell or 2-cell stage (67 %, 28 %, respectively), thereby, mirroring the results obtained with zygotes.

As expected from the proteasomal degradation of COPS3, the intensity of mCHERRY fluorescence declined as the injected zygotes reached the 2-cell stage (Figure 2D), however it was not completely abolished, as confirmed via LC-MS/MS (Supplementary Figure 2) and Western blotting (Figure 2E; the full-length blot is presented in Supplementary Figure 1). This observation was unexpected, because the 'Trim-away' reaction should be capable of acute and rapid protein degradation [21], as we indeed confirmed with another protein known to be depleted efficiently by 'Trim-away', SNAP23 [27] (Supplementary Figure 2). To tackle these contrasting results, we took advantage of a more stringent scheme of micromanipulation, as follows. We used 2-cell embryos preloaded with *mCherry-Trim21* mRNA, but we injected the RabMab® antibody in only one blastomere, while the other blastomere served as control. By comparing the sister blastomeres we confirmed that the proteasomal reaction had worked, since adding the culture medium with the potent cell-permeable proteasome inhibitor MG132 prevented the decrease of mCHERRY fluorescence in the blastomere that received the antibody (Supplementary Figure 2). More importantly, from the side-by-side comparison we saw that the proteasomal degradation of COPS3 was slow, having gone a small extent after 8 hours, and needing more than 24 hours to abolish the mCHERRY fluorescence (Figure 2F). The treated blastomere was arrested in

development, while the control blastomere progressed and formed a mini-blastocyst (Figure 2F), consistent with the effect of inhibiting COPS3 in whole embryos (Figure 2A-C).

Together, these findings strongly support the main conclusion of this study: COPS3 is required in mouse development much earlier than thought previously [6], that is, already after one zygotic division rather than at postimplantation. The contrasting behaviors of the sister blastomeres show that the requirement of COPS3 is cell-autonomous. However, the observed kinetics of the 'Trim-away' reaction is not up to the expectations [21], that is, neither rapid nor acute.

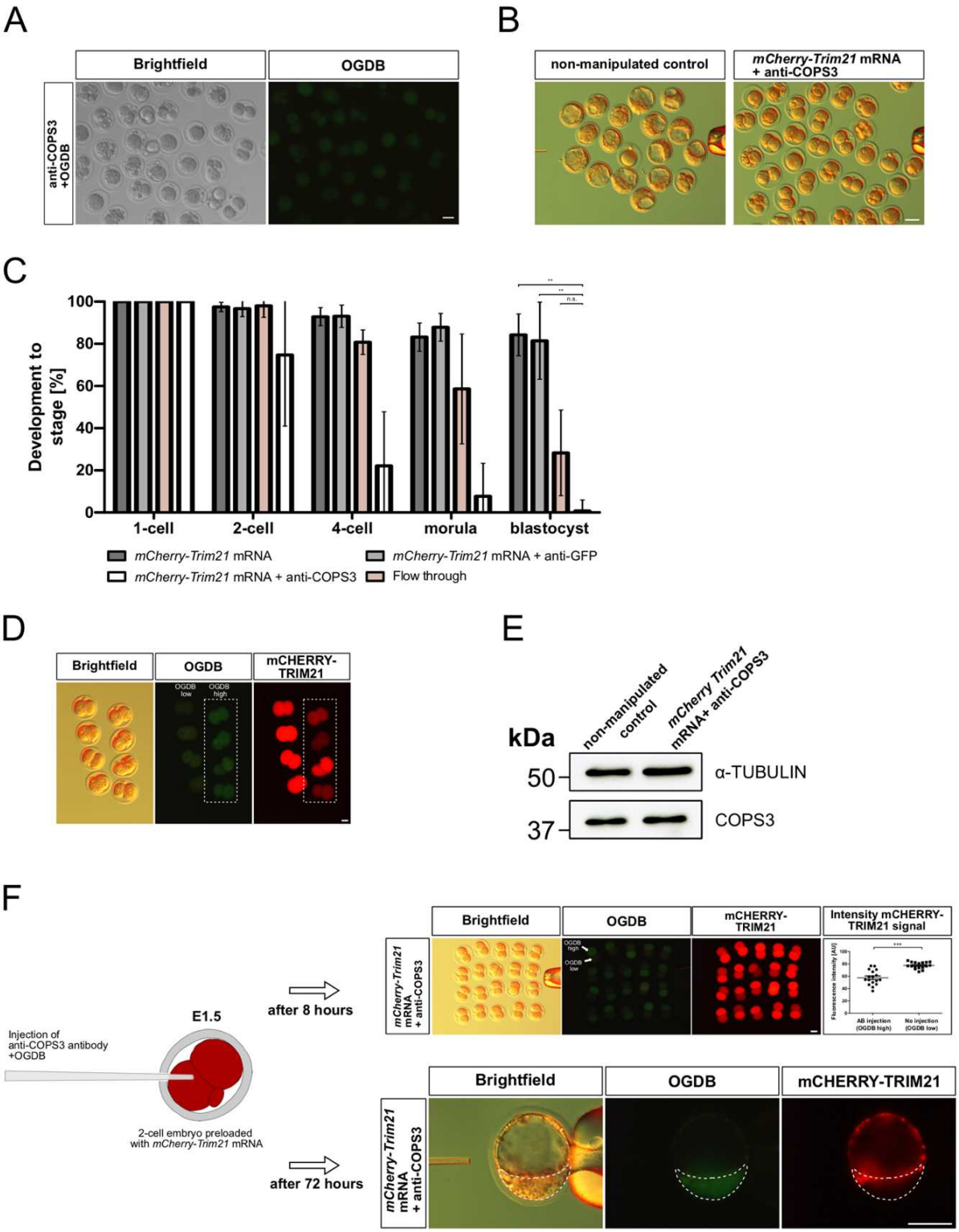

Figure 2. COPS3 is required for embryonic progression past the 2-cell stage in mice. (A). Representative brightfield images of zygotes (N = 48) which arrested after one cleavage when microinjected with anti-COPS3 antibody and OGDB, and formed no blastocysts (96 % blastocysts in control group, N = 28). Note that inert OGDB but not *mCherry-Trim21* mRNA was co-injected. **(B).** Representative images of zygotes (N = 285) which arrested after one cleavage when microinjected with *mCherry-Trim21* mRNA, anti-COPS3 antibody and OGDB, in contrast to the blastocyst progression of non-manipulated controls. **(C).** Developmental rates of zygotes microinjected with *mCherry-Trim21* mRNA (N = 212), *mCherry-Trim21* mRNA + anti-COPS3 antibody (N = 285), *mCherry-Trim21* mRNA + anti-GFP antibody (N = 245) or the buffer of anti-COPS3 antibody (1st flow of the antibody through the purification column, N = 99); data are presented as means and standard deviations, P values are calculated by t-test. **(D).** mCHERRY-COPS3 fluorescence intensity was reduced but not completely abolished by the TRIM21 reaction, as visualized in eight embryos, all of

which were preloaded with *mCherry-Trim21* mRNA at the 1-cell stage, but only the four embryos to the right also received COPS3 antibody 6 h after the mRNA (embryos in dotted box). Note that inert OGDB was co-injected, so as to identify *a posteriori* which embryos received only mRNA (OGDB low) and which embryos additionally received the antibody (OGDB high). **(E).** Western blot analysis (200 2-cell embryos) reveals that the total amount of COPS3 is not affected by TRIM21-mediated proteasomal degradation. The full-length blot is presented in Supplementary Figure 1. **(F).** Side-by-side comparison of the sister blastomeres, both preloaded with *mCherry-Trim21 mRNA* but only one receiving also the antibody (N = 20). The kinetics of the proteasomal degradation of COPS3 is slow, as visualized by mCHERRY fluorescence after 8 hours, which is completely abolished only after 72 hours. The blastomere fails to cleave further (dotted line). **, $P < 0.01$. Abbreviations: OGDB, Oregon-green dextran beads; n.s., not significant. Size bar: 50 µm.

COPS3's cortical deposit is largely insoluble and, thereby, unsuited for degradation by Trim-away unless the cortical rim is artificially destabilized

To reconcile the bold effect of COPS3 inactivation on embryo development (Figure 2A-C) with the slow kinetics of mCHERRY decline (Figure 2D-F), we considered that the protein substrate was refractory to degradation. This consideration is supported by two lines of evidence. Firstly, COPS3 remained present despite chemical extraction. Detergent Triton X-100 is known to extract the majority of oocytic proteins, except for those bound in fibrillar sheets (cytoplasmic lattices) or stable cortical structures [28-30] and is harsher than Tween 20. Consistent with the different strengths of the two detergents, the cortical rim of COPS3 withstood better the chemical extraction with 1 % Tween 20 than with 0.1 % Triton X-100 (Figure 3A). As a second line of evidence, the cortical rim of COPS3 withstood the block of protein turnover without any apparent change of intensity or thickness (Figure 3B) when oocytes were treated simultaneously with the two inhibitors cycloheximide (against protein synthesis) and MG132 (against protein degradation) for 72 h – a period of time spanning most of preimplantation development in mice. Thus, it is not sensible to expect that TRIM21-mediated proteasomal degradation could succeed where a harsh chemical treatment and a pharmacological block of protein turnover failed to disrupt the cortical rim.

We reasoned that if the nature of the endogenous COPS3 is what hindered the 'Trim-away' reaction, then an exogenous supply of monomeric COPS3 (i.e. not embedded in the holocomplex) should change the outcome and produce two clear effects: 1) expedite the kinetics of mCHERRY fluorescence decline; and 2) allow for complete degradation of the additional amount of COPS3. We overexpressed an engineered version of COPS3, imposed via microinjection of *mCherry-Cops3* mRNA into zygotes, thereby gaining the ability to resolve between endogenous and exogenous

COPS3, thanks to the mCHERRY epitope and the different molecular sizes of the native and engineered proteins. Immunofluorescent co-staining using RabMab® and anti-CHERRY antibodies reproduced the known picture of endogenous COPS3 (Figure 1D), but in addition, it showed that the exogenous COPS3 was mainly located in the nucleus, while only a weak signal visible in the cortical rim (Figure 3C). The latter is a remarkable observation, given the Triton X-100 stability of the rim. As the zygotes preloaded with *mCherry-Cops3* mRNA were injected with RabMab® antibody, the mCHERRY fluorescence was abolished (Figure 3D left) and in Western blot mCHERRY-COPS3 was depleted substantially from the amount which was built from *mCherry-Cops3* mRNA (Figure 3D right). However, also the endogenous COPS3 was depleted almost completely in the presence of exogenous COPS3 (Figure 3D right), in stark contrast to the behavior of endogenous COPS3 when tested alone (Figure 2D,E; the full-length blots of 2E and 3D are presented in Supplementary Figure 1). Thus, we conclude that exogenous COPS3 destabilized the cortical rim, and paved the way for augmented access of the 'Trim-away' reaction to the endogenous COPS3. Further, these results suggest that the cortical rim served as a slow-release source of COPS3 for functions in the nucleus (next section).

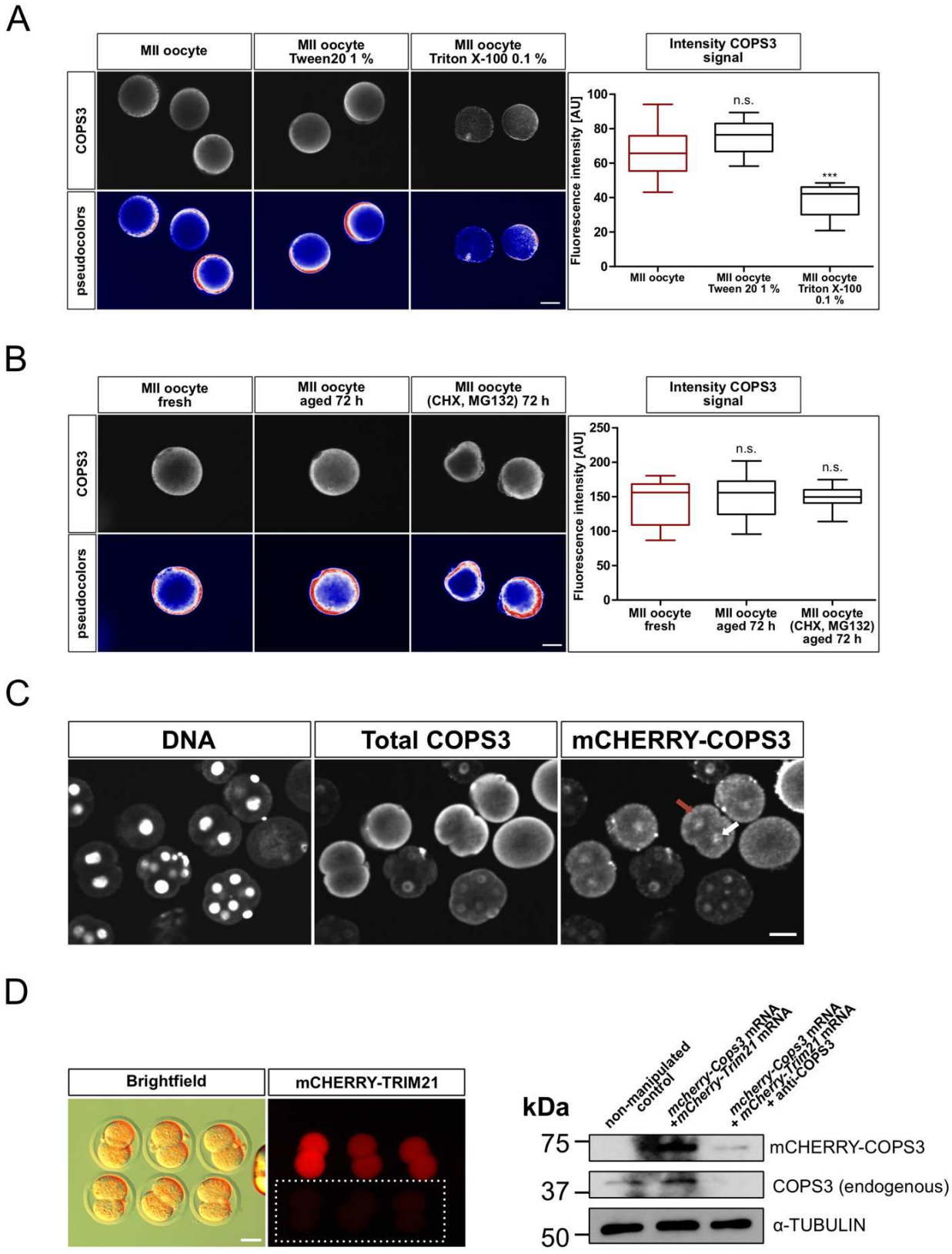

Figure 3. The cortical rim of COPS3 is refractory to spontaneous degradation and chemical extraction. (A). COPS3 is completely refractory to chemical extraction using Tween 20, and residues of COPS3 are seen also after extraction with Triton X-100. Compared to untreated oocytes, the cortical rim of COPS3 is still present, albeit thinned, in live oocytes extracted for 10 min with 1 % Tween 20 or 0.1 % Triton X-100 (N = 11, 11, 13, respectively). **(B).** COPS3 is refractory to spontaneous degradation, such as that taking place during oocyte aging *in vitro* in the presence of inhibitors of protein synthesis (CHX) and protein degradation (MG132) (MII fresh, n = 48; MII aged 72 h, n = 10; MII treated with CHX and MG132, n = 10). Representative images are shown, either raw or pseudocolored in Fiji using the

LUT 'Union jack.' Data in the box plots are presented as median, 1st and 3rd quartiles, and range (whiskers). P values are calculated by the Wilcoxon test, setting the MII oocyte as the reference (painted red in the plot). ***, P < 0.001. **(C).** Immunofluorescent co-staining of endogenous and exogenous COPS3 after overexpression of *mCherry-Cops3* mRNA. Images show that the exogenous COPS3 is mostly taken up in the nucleus (white arrow) but it also gains access to the cortical rim (red arrow). DNA was stained with YO-PRO-1. **(D)**. After overexpression of COPS3, the 'Trim-away' reaction attains effectiveness as revealed by loss of mCHERRY fluorescence in live-cell imaging (dotted box) and depletion of mCHERRY-COPS3 in Western blot. The full-length blot is presented in Supplementary Figure 1. Abbreviations: CHX, cycloheximide; MG132, proteasome inhibitor; n.s., not significant. Size bar: 50 μm.

COPS3 serves multiple functions and protects the nucleus from DNA damage in 2-cell stage embryos

To illuminate the functions of COPS3 and to identify the molecular basis for the 2-cell arrest observed after immunological COPS3 inhibition, we profiled the transcriptome of 2-cell embryos sampled at 24 h past the injection of COPS3 RabMab® antibody with or without TRIM21 (dataset GSE155205; Supplementary Table 2). Additionally, and as control, we profiled the influence of *Trim21* mRNA over-expression on the transcriptome. We set the non-manipulated embryos as the reference, as these are the most distinct in phenotypic and molecular terms from all other experimental groups (out-group comparison). It is reassuring that the 2-cell stage transcriptome was minimally impacted by the microinjection and the overexpression of *Trim21* mRNA, compared to the non-manipulated group (22 mRNAs, or 0.08 %, were differently expressed; fold change ≥ 2, $p \leq 0.01$, t-test; Figure 4A).

When TRIM21 was combined with the COPS3 RabMab® antibody, it induced a vast perturbation of the transcriptome, even though the COPS3 depletion was partial: We found an altered (≥ 2-fold, $p \leq 0.01$) expression of 1280 mRNAs, of which 1185 mRNAs were unique for the depletion, 91 mRNAs were shared with the antibody-alone group, and 4 were shared with the *Trim21* mRNA only group (Figure 4B). Compared to the 1280 mRNAs of the RabMab® antibody with TRIM21, the antibody alone perturbed 236 mRNAs, of which 145 mRNAs were unique for this group. It, thus, appears that the 2-cell phenotype is due, to a minor extent, to antigen-based masking (antibody alone) and, to a major extent, to antigen removal (TRIM21-mediated proteasomal degradation). In total, aggregating the results and discarding the duplicates, 1421 mRNAs (n = 145 + 91 + 1185) were perturbed by anti-COPS3 with or without TRIM21. These significantly perturbed mRNA did not include *Cops3* itself, thereby indicating that acting on COPS3 did not induce a compensatory transcriptional response at this locus.

We subjected the set of 1421 mRNAs to GO analysis, using the software ReViGO to aggregate and visualize the GO enrichment results [31]. ReViGO returned a large number of hits related to a large number of biological processes and sub-compartments of the cell, for example ranging from 'nuclear part' (GO:0044428) to 'cytosolic part' (GO:0044445), and from 'DNA repair' (GO:0006281) to 'translation' (GO:0006412). The most prominent hits were those related to RNA metabolism (Figure 4B). Having found this process is consistent with the window of time of this study, when degradation of (certain) maternal mRNAs is required shortly after fertilization in order to enable *de novo* transcription during the embryonic genome activation (EGA) [32] at the 2-cell stage. In a nutshell, this is the window of time of the maternal-to-embryonic transition. We, therefore, compared and contrasted the 1421 mRNAs with a list of mRNAs that are known to be degraded (oocyte-specific, n = 149) or upregulated (major wave of EGA, n = 3480) in 2-cell mouse embryos (Datasets S1 and S6 in [33]). Only 8 of the 149 oocyte-specific mRNAs (5.4 %) were found among the 1421 COPS3-regulated mRNAs (0.6 %), while 503 of the 3480 EGA-controlled mRNAs (14.5 %) were found among the 1421 COPS3-regulated mRNAs (35.4 %), in the sense that COPS3 depletion prevented the upregulation otherwise experienced by these mRNAs at the 2-cell stage. Strikingly, the reference list of EGA-regulated mRNAs [33] includes so-called 'housekeeping' genes that were recommended for mouse embryos based on expression stability across preimplantation stages [34]. Thus, the maternal-to-embryonic transition may account for 511 (n = 8 of the 149 + 503 of the 3480, see above) of the 1421 mRNAs which are regulated by COPS3, but it does not explain the rest of them (n = 1421 – 511). As can be seen, our GO analysis returned a broad variety of terms, reminiscent of an effect on a general and basic function of the cell (including the 'housekeeping' ones), such as a basic capacity for RNA, DNA and protein synthesis, which can be affected when maternal factors are removed from oocytes [35].

Therefore, we examined the capacity of COPS3-depleted 2-cell embryos for total RNA, DNA and protein synthesis, as determined by Click-IT chemistry after the incorporation of the respective precursors in cultured embryos. In contrast to unchanged protein and RNA synthesis (Figure 5A, B), DNA synthesis was significantly higher (2X) in COPS3-depleted 2-cell embryos relative to control embryos (Figure 5C), in conjunction with a significant increase in the number of DNA double-strand breaks inferred from the number of histone γH2A.X nuclear foci [14] (Figure 5D). Given the factor 2X, we hypothesized that the increased DNA content was due to DNA endoreduplication, and that the increased DNA damage might be a manifestation of replication stress, possibly in conjunction with reduced levels of genes that superintend to DNA repair. We went back to our transcriptome data

to look for relevant changes in related gene activities to corroborate or confute this hypothesis. In line with the latter, the levels of *Geminin* mRNA – the factor required to prevent endoreduplication – are significantly reduced in the COPS3-depleted 2-cell embryos relative to control embryos (– 88 %, p = 0.02; Figure 5E); whereas the levels of *CyclinE2* mRNA – the factor required to permit endoreduplication [36] – are increased (+ 80 %, p = 0.06). The increased number of DNA double-strand breaks is ascribed to insufficient DNA damage response, since our transcriptome data show that 7 of the 10 DNA repair genes which have a lethal mutant phenotype during preimplantation [4] are significantly less expressed in COPS3-depleted 2-cell embryos relative to control embryos (*Ercc2*, -76 %, p = 0.08; *Dcaf2*, -86 %, p = 0.03; *Pcna*, -64 %, p = 0.004; *Rpa1*, 0 %, p = 0.95; *Wee1*, -59 %, p = 0.02; *Nop53*, -82 %, p = 0.01; *Cdk1*, -89 %, p = 0.02; *Plk1*, -83 %, p = 0.002; X*ab1*, -77 %, p = 0.02; *Pot1a*, -18 %, p = 0.22; t-test; Figure 5E). This observation can be extended to the transcripts of two additional, well-known DNA repair activities (i.e. *Rad21*, -60 %, p = 0.02; *Brcc3,* -43 %, p = 0.04; t-test; Figure 5E). Some of the mRNAs above were also confirmed as proteins. Specifically, the proteins of *Geminin* and *Brcc3* were detected in unmanipulated and in *Trim21* mRNA-injected embryos but not in COPS3-depleted embryos (see LC-MS/MS data in Supplementary Table 1), consistent with the significant reduction of the two mRNAs (-88 %, -43 %). We could not verify the stable levels of the mRNAs of 'housekeeping' genes [34] in COPS3-depleted 2-cell embryos, consistent with the report that these genes are not constantly expressed but, in fact, regulated [33].

Together, these data provide the molecular rationale for the phenotypic consequences of immunological COPS3 inactivation. This inactivation elicits a wide range of changes in the biological processes, including housekeeping, many of which would suffice on their own to affect the viability of 2-cell embryos. In particular, we observe that the nuclear processes of DNA replication and repair of DNA are affected (endoreduplication + histone γH2A.X nuclear foci) and this takes place in parallel with the observation of nuclear relocalization of the cortical deposit from the 2-cell stage onward.

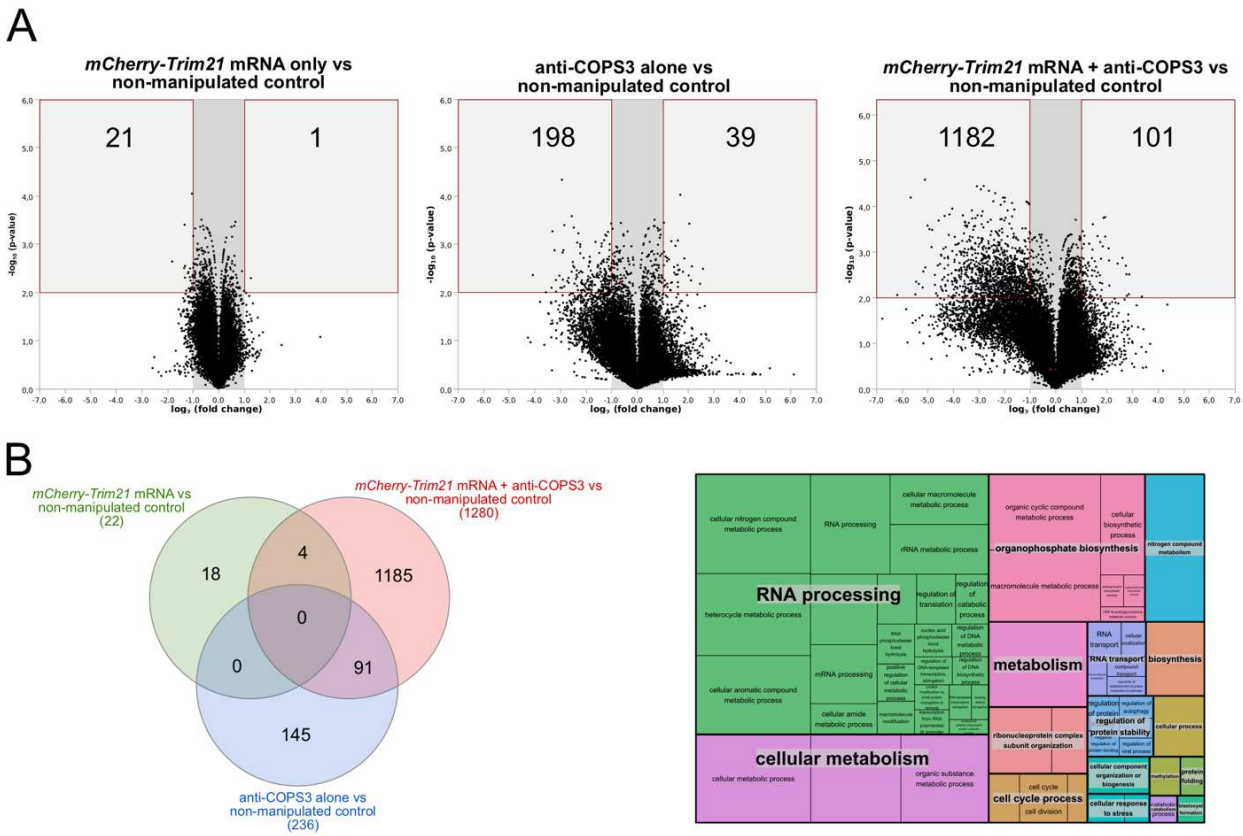

Figure 4. TRIM21-mediated COPS3 inactivation but not TRIM21 brings about a large perturbation of gene expression at the 2-cell stage. (A). Volcano plots show the effect of TRIM21 (left), COPS3 antibody (center) and TRIM21+antibody (right) on the embryo transcriptome at the 2-cell stage. The data point of *Cops3* mRNA is painted red. The numbers of mRNAs that are under- vs. over-expressed (fold change ≥ 2, p ≤ 0.01, t-test.) are shown in the upper corners. **(B).** (Left) Venn diagram recapitulating the number of transcripts that are differently expressed in either direction – up or down (fold change ≥ 2, p ≤ 0.01, t-test) as a result of the same treatments that were compared pairwise in the volcano plots. (Right) TreeMap view of the 1421 mRNAs identified by the Venn diagram. Each rectangle is a single cluster representative. The representatives are joined into 'superclusters' of loosely related terms, visualized with different colors. The size of the rectangles was adjusted to reflect the number of the gene ontology terms in the cluster representative.

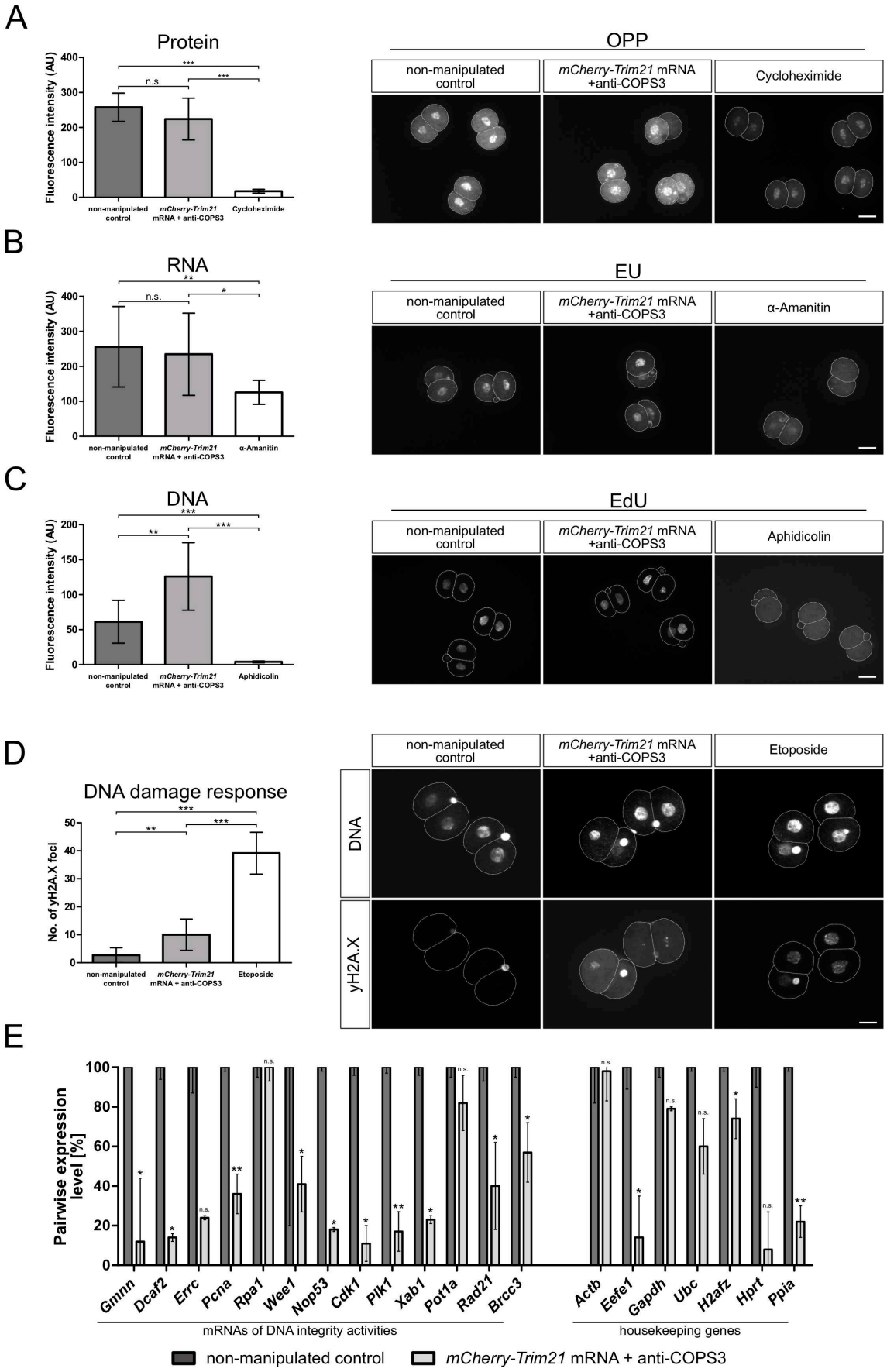

Figure 5. DNA is affected by antibody-mediated COPS3 inactivation but not RNA or protein synthesis. (A). Histogram (left) and representative pictures (right) show that COPS3-inactivated zygotes incorporated the OPP precursor for

protein synthesis to the same extent as non-manipulated controls, while the protein synthesis inhibitor cycloheximide reduced the incorporation (N = 12, 14, 11, respectively). **(B).** COPS3-inactivated zygotes incorporated the EU precursor for RNA synthesis to the same extent as non-manipulated controls, while the RNA polymerase II inhibitor α-amanitin reduced the incorporation (N = 5, 6, 4, respectively). **(C).** COPS3-inactivated zygotes incorporated the EdU precursor for DNA synthesis to a higher extent than non-manipulated controls, while the DNA polymerase inhibitor aphidicolin reduced the incorporation (N = 5, 7, 11, respectively). **(D).** COPS3-inactivated zygotes presented more histone γH2A.X foci per nucleus than non-manipulated controls, while the topoisomerase inhibitor etoposide increased the number of foci even more (N = 11, 11, 8, respectively). **(E).** Transcript levels of key genes involved in the prevention of DNA endoreduplication and actuation of DNA double-strand break repair as well as housekeeping genes (from transcriptome data, dataset GSE155205; Supplementary Table 2). Data are presented as means and standard deviations. P values are calculated by t-test. *, $P < 0.05$. **, $P < 0.01$. ***, $P < 0.001$. Abbreviations: wt, wildtype; OPP, O-propargyl-puromycin; EU, 5-ethynyl uridine; EdU, 5- ethynyl-2'-deoxyuridine; ns, not significant. Size bar: 50 μm.

Discussion

So far, COPS3 has been understood mainly as a factor necessary for epiblast survival at the time of mouse embryo implantation [6] – a role shared with other mutated members of the COP9 signalosome complex i.e. COPS2, COPS5, COPS6 and COPS8 [37-40]. The results of our immunological COPS3 inactivation reveal that prior to supporting epiblast survival in the postimplantation embryo, COPS3 accumulates in the oocyte and is required for protecting DNA integrity during the 2-cell stage. *Cops3* is thereby recruited to the group of only 10 genes (reviewed in [4]) which have a lethal mutant phenotype caused by defective DNA repair during the very early phase of development that harbors cellular totipotency. The reassigned function of COPS3 is mediated by an abundant, stable and hitherto overlooked protein deposit, which is present in oocytes in the form of a cortical rim – a cytological theme found also in maternal genes such as those of the subcortical maternal complex (SCMC) [41,42]. The rim is mostly insoluble and, thereby, unsuited for degradation by the 'Trim-away' method in its conventional form, but it coexists with a less abundant fraction in the nucleus, which is the actual point of use of COPS3 in early mouse embryos.

Embryonic arrest at the 2-cell stage after co-injection of anti-COPS3 antibody with or without *Trim21* mRNA is a phenotype which is reminiscent of so-called maternal-effect genes, such as *Mater (Nlrp5)*, *Zar1*, *Hsf1* and *Brg1 (Smarca4)* [43-46]. However, *Cops3* is known to function in germinal-vesicle mouse oocytes to support meiosis [17], whereas mutations of maternal-effect genes should affect the embryogenesis without affecting the gametogenesis (neither oogenesis nor spermatogenesis) [47]. Looking for the main cause of the 2-cell arrest following immunological COPS3-inactivation proved challenging because it turned out that COPS3 is involved in numerous molecular functions of many different cellular processes. Recalling the case of *Brg1* was helpful to look for a cause in the case of *Cops3*. When *Brg1* was deleted in mouse oocytes [46], the arrested 2-cell embryos were affected in about 30 % of the α-amanitin-sensitive genes, which are *bona fide* markers of EGA. For this reason, we interrogated the transcriptome of COPS3-inactivated embryos. It is reassuring that the number of mRNAs which were perturbed by the microinjection of the sole *Trim21* mRNA was very small, given the known interaction partners of TRIM21, for example, the gap-junction subunit CONNEXIN 43 [48], the tumor suppressor p53 [49] or the histone deacetylase HDAC6 [50]. By contrast, the transcriptome was vastly perturbed – including 'housekeeping' mRNAs – after COPS3 inactivation, and such vastness requires an explanation. The gene *Cops3* has paralogs whose proteins take part in the proteasome lid and the translation

initiation complex, for example, *Psmd3* [51,52]. These complexes determine the fate of hundreds of proteins and, therefore, malfunctioning of each can cause the failure of many cellular processes, including basic biosynthetic ones – among these, DNA metabolism.

Among the many things that can go wrong predictably because of COPS3-inactivation, given the gene ontologies associated with this gene, the embryos had a doubled DNA content with an increased number of histone γH2A.X foci, while RNA and protein synthesis remained unchanged. The double DNA content *per se* may not be blamed for the 2-cell arrest of COPS3-inactivated embryos, since tetraploid embryos form blastocysts [53], whereas genotoxic stress (DNA damage) is well-known to cause 2-cell arrest [54]. Similar effects on DNA replication and repair in 2-cell mouse embryos have previously been reported after genetic ablation of *DDB1- and CUL4-associated factor 2* (*Dcaf2*) and *Cullin 1* (*Cul1)* [55-58], however, the operating mode of COPS3 may or may not be the same. Whereas the inactivation of CUL1 resulted in an accumulation of pan-CYCLIN E [55], the inactivation of COPS3 resulted in an accumulation of Cyclin E2 mRNA but not of Cyclin E1 mRNA; and whereas COPS3 features a cortical deposit in oocytes, this structure could not be demonstrated in *Dcaf2*-deficient oocytes (due to the lack of a suitable antibody) and the microinjection of *mCherry*-tagged *Dcaf2* mRNA in oocytes did not result in the assembly of a cortical rim [56]. Refining the mechanistic picture of the role of COPS3 in DNA metabolism, our study also indicated possible mediators of the nuclear DNA phenotype: Downregulation of genes such as *Geminin* and *Brcc3*, which superintend to DNA endoreduplication and DNA repair, respectively. Together, these novel findings abide by the notion that maintenance of genome integrity is a precondition for totipotency [59], documented in numerous cases, for example, the perturbation of totipotency marker genes (e.g. *Zscan4d*) leading to genomic instability and karyotype abnormalities [60].

In spite of the 2-cell lethality of COPS3 inactivation, this phenotype originated from a partial depletion: Only a minute fraction of the total COPS3 was depleted, while most of it was still there. As we are going to discuss, this was not an experimental, but a biological issue, linked to the stability and accessibility of the cortical rim of COPS3. However, this is a potential limitation of our study that prompts at least two questions: 1) Why was the depletion partial and 2) how could a partial depletion be so detrimental? To answer the first question, we recall that oocytes' structures persisting during preimplantation embryos and even after extraction with detergents have been known for a long time, such as cytoplasmic lattices and SCMC [29,30,61], which are subcortically located in the ooplasm similar to COPS3. The cortical rim of COPS3 withstood the

extraction with Tween 20 and Triton X-100. This gave us the idea to introduce an additional amount of COPS3 into the cell, via microinjection of *Cops3* mRNA (overexpression), in order to create a free pool which should be more accessible for the 'Trim-away' reaction. Not only was the exogenous amount of COPS3 depleted efficiently, but this happened also to the endogenous COPS3. It thus appears that the exogenous COPS3 had destabilized the endogenous COPS3, allowing TRIM21 and antibody to gain access to both. In addition, we appreciated a distinct localization of exogenous COPS3 also in the nucleus. This observation leads us to envisage an apportionment of total COPS3 in two pools: One pool is sequestered (insoluble) in the cortical rim and is, thus, not accessible for enzymatic proteolysis, the other pool is soluble in the cytosol, from where it can also access the nucleus and operate in it. To answer the second question, namely how a partial depletion could be so detrimental, we propose that the rim is not the point of use of COPS3 in the early embryo, and that COPS3 in the rim cannot be easily transported to the 2-cell nucleus – where its function is first needed, as revealed by our DNA assays. The nuclear amount is very small and this would be why our Western blot analysis of the total native amount (no overexpression) was unable to detect change after TRIM21-mediated proteasomal degradation of COPS3. This consideration elicits a speculation that the phenotype is not controlled by the total resource of COPS3 present but by the part of it needed at the point of use (limiting factor) – reminiscent of the 'law of the minimum' formulated by Justus von Liebig in the 19th century [62]. From drawing this parallel, we can better understand the idea that an authentic phenotype can be exposed by acutely reducing – but, in fact, not completely removing – gene activity [63], since only a fraction of the total is biologically relevant and the biological system had no time to mount adaptive responses (not to mention the phenotypes that may otherwise remain hidden due to loss-of-function embryonic lethality [64]). Together, these two answers predict that a complete depletion by TRIM21-mediated proteasomal degradation may not work, and may not be required to work (depending on one's aim), for every protein. Indeed, it may be noted that out of thirteen studies which applied the TRIM21-mediated proteasomal degradation on oocytic or embryonic proteins in mammals [21,22,27,65-74], four studies reported complete depletion (ITPR1 [67]; SNAP23 [27]; G6PD, PKM, GFPT1 [65]; EG5 also known as KIF11 [21]), four studies reported almost complete depletion (BTG4 [68]; TACC3 [69]; RACGAP1 also known as CYK4 and PLK1 [70]; SMC3 [72]) and five studies reported incomplete depletion (RCC1 [66]; CENPF [71]; TEAD4 [22]; aPKC also known as PRKC [73]; HUWE1 [74]). Thus, complete removal of the protein of interest seems to be more the exception than the rule (with current technology).

In conclusion, totipotency is generally regarded as a special property which hinges on extraordinary and elusive 'master' genes. We have recruited COPS3 – hitherto known for serving rather ordinary, basic, not to say 'housekeeping' duties – to the family of maternal (but not maternal-effect) factors that are necessary to protect genome integrity during the totipotent phase, i.e. the 2-cell stage of mouse embryo development. The case of *Cops3* is probably not limited to this gene. Similar to *Cops3*, also *Sox2* and *Max* had null (-/-) blastocysts with the same immunostaining intensity as +/- or +/+ counterparts after intercross of heterozygotic parents [6,75,76], suggestive of relevant oocytic deposits persisting until the stage of embryo implantation. Similarly, the proteins of the SCMC genes were found to be still present at the blastocyst stage, as revealed by Western blotting, although the alleles had been inactivated in the zygote and the transcripts degraded at the 2-cell stage [42]. More recently, immunofluorescence revealed that the pyruvate dehydrogenase complex translocated from the cytoplasm to the nucleus of the 2-cell stage mouse embryos, and this translocation was necessary for EGA [77]. The common trait in these various cases was that new insight came from direct inspection of the protein products of those genes, thereby, questioning the safety of transcriptomic screening to identify the molecular signature of totipotency, since this signature could be partially made of proteins, which escape transcriptomic screening. This advises us that gene role assignments in embryogenesis may be less safe than assumed when the proteins of those genes are accumulated in oocytes, and suggests that further identification of key maternal proteins and their functions via single-cell proteomics and 'Trim-away', respectively, could greatly facilitate studies of totipotency. However, we need to be aware of the prerequisites posed by this still young method, beyond the availability of excellent antibodies: A quantitative knowledge of the oocyte proteome and of its subcellular distribution.

Methods

Compliance with regulations on research animals. Mice were used for experiments according to the license issued by the Landesamt für Natur, Umwelt und Verbraucherschutz of the State of North Rhine-Westphalia, Germany (license number 81-02.04.2017.A432), in accordance with the procedures laid down in the European Directive 2010/63/EU. We observed the ARRIVE guidelines [78] to the extent applicable. All mice were maintained in individually ventilated cages in the animal facility of the MPI Münster, with a controlled temperature of 22 °C, a 14/10 h light/dark photoperiod and free access to water and food (Harlan Teklad 2020SX).

Mouse oocyte and embryo production. To collect MII oocytes, six- to eight-week-old B6C3F1 females were each primed with 10 I.U. pregnant mare serum gonadotropin (Pregmagon, IDT) and human chorionic gonadotropin (Ovogest, Intergonan) injected intraperitoneally 48 h apart. The cumulus-oocyte complexes were recovered from the oviducts at 9 am on the day following hCG injection, and dissociated in hyaluronidase (50 I.U./mL in Hepes-buffered CZB (HCZB) medium). The cumulus-free oocytes were cultured in α-MEM medium (Sigma, M4526), until further use. To produce fertilized oocytes (zygotes, pronuclear-stage) *in vivo*, the gonadotropin-primed females were mated to CD1 stud males. On the morning of the vaginal plug, the cumulus-oocyte complexes were recovered, dissociated as described, and the zygotes were cultured in 500 µL of Potassium (K) simplex optimization medium containing free aminoacids (KSOM(aa)), in a four-well Nunc plate without oil overlay, at 37 °C under 6 % CO_2 in air. To produce parthenogenetic embryos, MII oocytes were activated in Ca-free α-MEM medium containing 10 mM $SrCl_2$ and 5 µM Latrunculin B, for 6 h. Following activation, the pronuclear-stage oocytes were washed in KSOM(aa) in three steps of 10 min each, to remove intracellular accumulated Latrunculin B. Parthenotes were cultured in 4-well plates containing 500 µl KSOM(aa) medium at 37°C (6% CO_2). KSOM(aa) was synthesized from individual components and included 0.5X EAA, 0.5X NEAA and 0.5X glutamine according to recipe [79]. Culture media α-MEM and KSOM(aa) were also added with 0.2% (w/v) bovine serum albumin and gentamicin (50 I.U./mL).

Proteome and transcriptome analysis of oocytes, zygotes and preimplantation embryos. To assess the developmental profile of COPS3 we made use of already existing datasets that we had published previously [22,26]. To assess the immediate impact of TRIM21-mediated COPS3 depletion on the protein composition of the 2-cell stage we generated a new proteomic dataset using the

same pipeline as described in [22]. The only difference to the previous pipeline was the use of a more recent version of MaxQuant (1.6.1.7.0) as well as the inclusion of deamidation at N-terminus as additional variable modification. Samples were comprised of 200 two-cell embryos in each of five groups: non-injected i.e. non-manipulated control (group 1), injected with OGDB (group 1.1), injected with *mCherry-Trim21* mRNA and OGDB (group 2), injected with *mCherry-Trim21* mRNA, OGDB and anti-COPS3 antibody (group 3), injected with OGDB and anti-COPS3 antibody (group 4), and each group was produced as unique specimen. To assess the consequences of COPS3 depletion on embryonic gene expression at the 2-cell stage we generated a new transcriptomic dataset using the same pipeline as described in [5]. Samples were comprised of 100 two-cell embryos in each of four groups: non-injected i.e. non-manipulated control (group 1), injected with *mCherry-Trim21* mRNA and OGDB (group 2), injected with *mCherry-Trim21* mRNA, OGDB and anti-COPS3 antibody (group 3), injected with OGDB and anti-COPS3 antibody (group 4), and each group was produced in duplicate. Differently expressed transcripts were represented graphically using InteractiVenn [80] and imported in ReViGO [31] for GO analysis.

Immunofluorescence analysis of COPS3, COPS5, mCHERRY and γH2A.X expression. Oocytes or embryos were analyzed by performing an immunostaining followed by confocal microscopy imaging, as per our routine protocol [81]. The following primary antibodies were applied to the specimens overnight at 4 °C: two anti-COPS3 rabbit IgGs (Abcam 79698; RRID:AB_261850), anti-COPS5 (NOVUS BIO JAB1 2A10), anti-mCHERRY (NOVUS BIO NBP1-96752), anti-histone γH2A.X (Cell Signaling #80312), in dilutions of 1:250 (Abcam 79698), 1:50 (RRID:AB_261850), 1:350 (NOVUS BIO JAB1 2A10), 1:500 (NOVUS BIO NBP1-96752), 1:400 (Cell Signaling #80312). Appropriate Alexa Fluor-tagged secondary antibodies (Invitrogen) were matched to the primaries and incubated for 1-2 h at room temperature. DNA counterstaining was performed with YO-PRO-1 (1 µM). For imaging, embryos were placed in 5 µl drops of PBS on a 50-mm thin-bottom plastic dish (Greiner Bio-One, Lumox hydrophilic dish; Frickenhausen, Germany) and overlaid with mineral oil (M8410 Sigma). Images were captured on the stage of an inverted microscope (Eclipse 2000-U; Nikon, Düsseldorf, Germany) fitted with a spinning disk confocal unit (Ultra View RS3; Perkin-Elmer LAS, Jügesheim, Germany). A Nikon Plan Fluor 20X /0.75 N.A. multi-immersion objective was used. Twenty optical sections per embryo were captured using a Hamamatsu ORCA ER digital camera (Hamamatsu Photonics KK, Japan). Maximum projections were analyzed with Fiji (ImageJ version 2.0.0-rc-69/1.52p).

Block of oocyte's protein turnover or chemical extraction with detergents. MII oocytes were subjected to either of these two treatments, as follows. To block protein turnover, oocytes were cultured for 3 days in α-MEM supplemented with inhibitor of protein synthesis (cycloheximide 50 µg/mL [82]) and inhibitor of proteasomal activity (MG132, peptidaldehyde Z-Leu-Leu-Leu-CHO, 10 µM [83]). The proteasome inhibitor was also applied alone on 2-cell embryos to demonstrate that the TRIM21 reaction depends on proteasome function. For chemical extraction, MII oocytes were treated with buffer containing 0.1M KCl, 20 mM $MgCl_2$, 3 mM EGTA, 20 mM HEPES (pH 6.8), 1 x Complete Protease Inhibitor Cocktail (Roche) and 0.1% Triton X-100 or 1% Tween 20 for 10 min [61]. After each treatment, embryos were fixed with 3.7% formaldehyde for 15 min, and processed for immunofluorescence and imaging as described (see "Immunofluorescence analysis of COPS3, COPS5, mCHERRY and γH2A.X expression"). The native images were normalized using identical settings for contrast and brightness for reasons of comparability before being used for analysis. Images were pseudocolored for demonstration (not for analysis!) purposes [84-86]. A 'Union Jack' LUT color palette was used, as provided from the LUT archive of Fiji (ImageJ version 2.0.0-rc-69/1.52p).

mCherry-Trim21 **mRNA preparation for TRIM21-mediated protein depletion, and** ***mCherry-Cops3*** **mRNA preparation for COPS3 overexpression.** An *mCherry-mTrim21* expression construct built on plasmid pGEMHE was obtained from Melina Schuh (Addgene plasmid # 105522). A *mCherry-Cops3* expression construct was generated by inserting mouse *Cops3* coding sequence (NCBI Reference Sequence: NM_011991.1) into pGEMHE-mCherry-mTrim21 using EcoRI (5′ cloning site) and NotI (3′ cloning site). The result is a fusion protein with mCHERRY at the C-terminal of COPS3. For *in vitro* transcription, plasmids were linearized with SwaI (ThermoFisher, cat. no. FD1244). Capped mRNA was synthesized with T7 polymerase (Ambion mMessage mMachine T7 kit) according to manufacturer's instructions. Obtained mRNAs were purified with Quick-RNA MicroPrep (Zymo Research, cat. no.: R1051) and preserved in MilliQ water at -80 °C.

Microinjection of mRNA and antibody in oocytes, zygotes or blastomeres. MII oocytes or zygotes were injected at approximately 15 h post-hCG with a mixture of mRNA, dextran beads fluorescently labeled with Oregon Green (OGDB; 70 kDa; ThermoFisher cat. no. D7173) and antibody at the final concentration of 0.2 mg/mL, 0.017 mg/mL and 0.5 mg/mL, respectively, dissolved in MilliQ water. Antibodies were rabbit monoclonal anti-COPS3 (AbCam 79698), mouse monoclonal anti-COPS3 (Developmental Studies Hybridoma Bank Cat# PCRP-COPS3-2D9,

RRID:AB_261850) and anti-GFP (Thermo Fisher MA5-15256 (GF28R)). For cell injection, antibodies were washed four times and concentrated at 4 °C using Amicon Ultra-0.5 100 KDa centrifugal filter devices (Merck Millipore, cat. no. UFC100) to remove salts and preservatives (e.g. sodium azide) and stabilizers (e.g. albumin), and to replace the buffer with water. In case of blastomere injection, zygotes were preloaded with a mixture of mRNA and dextran beads without antibody, followed by the antibody on the next day at approximately 39 h post-hCG. Microinjection was conducted on the stage of a Nikon TE2000U microscope fitted with a piezo drill (PrimeTech), using a blunt-end glass needle (inner diameter 6-7 microns, outer diameter 8-9 microns) filled with 2-3 microliters mercury at the tip. Volumes were pressure-injected into the zygote or blastomere using a Gilmont GS-1200 micrometer syringe operated manually. During the microinjection, cells were kept in a 200-300 microliters drop of Hepes-buffered CZB medium [87] on a glass-bottomed (Nomarski optics) dish at a room temperature of 28 °C. After microinjection, zygotes or embryos were allowed to recover in the drop for 5–10 min, before returning them to KSOM(aa) medium.

Immunoblotting analysis of COPS3, mCHERRY and SNAP23. Oocytes or embryos were centrifuged in protein-free HCZB medium at 700 rpm for 10 min to form a tiny pellet. The supernatant was carefully aspirated using a mouth-operated micropipette, and replaced by RIPA buffer containing protease inhibitors. The resultant lysates were mixed with 6x Laemmli sample buffer and boiled for 5 min at 99 °C. These samples were loaded on a 12 % separation gel and blotted onto a PVDF membrane. The membrane was blocked for at least 3 h and incubated (3 % nonfat dry milk in 0.1 % PBS-Tween) with primary antibodies overnight at 4 °C. After 3X washing in 0.1 % PBS-Tween, the blot was incubated with horseradish peroxidase (HRP)-coupled secondary antibody at RT for 1 h. The membrane was washed and then developed with chemiluminescent HRP substrate solution. The chemiluminescent signal was detected using the AGFA Curix 60. Signal intensities were standardized on α-Tubulin (1:5000, Merck, Cat. no.: T6199). The antibodies against the proteins of interest (COPS3, AbCam 79698; mCHERRY, NOVUS BIO NBP1-96752; SNAP23, Fisher PA1-738) were applied at a dilution factor of 1:20000.

Assays for DNA, mRNA and protein synthesis. For detecting DNA, mRNA and protein synthesis in two-cell stage blastomeres, 5-ethynyl-2'-deoxyuridine (EdU), 5-ethynyl uridine (EU) and O-propargyl-puromycin (OPP) were used, respectively. The detection of incorporated EdU was performed using Click-iT EdU Alexa Fluor 647 imaging kit (Invitrogen, Cat. No. C10340) according to the manufacturer's protocol. The detection of incorporated EU was performed using Click-iT

EU Alexa Fluor 594 imaging kit (Invitrogen, Cat. No. C10330) according to the manufacturer's instruction. The detection of incorporated OPP was performed using Click-iT EdU Alexa Fluor 647 imaging kit (Invitrogen, Cat. No. C10458) according to the manufacturer's protocol. For the incorporation of EdU, the culture medium KSOM(aa) was supplemented with 10 µM final concentration EdU for 16 h overnight. For control, embryos were cultured with additional 2.5 µg/mL Aphidicolin for 16 h overnight. For the incorporation with EU, the culture medium containing 1 mM EU was used for culturing embryos for 3 h. For control, embryos were cultured with additional 100 µg/mL α-Amanitin for 4 h. For the incorporation of OPP, the culture medium KSOM(aa) was supplemented with 20 µM final concentration OPP for 3 h overnight. For control, embryos were cultured with additional 50 µg/mL cycloheximide for 16 h overnight. Following this procedure, all embryos were then fixed with 3.7% formaldehyde for 15 min, followed by a 0.5% Triton X-100 permeabilization step for 15 min at room temperature and then incubated with the Click-iT reaction cocktail for 30 min protected from light. Images were taken on a Nikon TE2000 microscope fitted with an UltraView RS3 confocal module.

Statistical analysis of developmental rates, image data and gene expression data. Developmental rates and fluorescence intensities were analyzed by two-tailed Student's *t* tests using the statistical program JMP v.13 (SAS). Microarray data analysis was performed in-house using the output of the Affymetrix Expression Console and Transcriptome Analysis Console, exported in Microsoft Excel format and imported in JMP version 13. Proteome data analysis was performed in-house using the iBAQ output of MaxQuant Software version 1.6.2.10, exported in Excel format and imported in JMP version 13.

Additional information

Ethics declaration for human experiments and consent for publication

Not applicable

Ethics declaration for animal experiments

See Methods section.

Availability of data and material

All data generated or analyzed during this study are included in this published article as Summary tables (Supplementary Information files).

Supplementary table 1: Proteome analysis of 2-cell mouse embryos subjected to immunologic COPS3 inactivation. https://figshare.com/s/0b53be9432b41fbd2e30

Supplementary table 2: Transcriptome analysis of 2-cell mouse embryos subjected to immunologic COPS3 inactivation. https://figshare.com/s/e9d74e21c22b6611494b

The raw data of supplementary table 1 (mass spectrometry) have been deposited to the ProteomeXchange Consortium via the PRIDE partner repository [88,89] with the dataset identifier PXD017212. The raw data of supplementary table 2 (transcriptome analysis) have been deposited in the NCBI's Gene Expression Omnibus and are accessible through GEO Series accession number GSE155205.

For additional datasets cited in this study (PXD012613, DNA Databank of Japan Sequence Read Archive DRA005956 and DRA006335) we refer to the original publication [26].

Competing interests

The authors declare no competing interests.

Funding

This study was supported by the Deutsche Forschungsgemeinschaft (grant DFG BO-2540/4-3 to M.B. and grant FU-583/5-1 to G.F.).

Authors' contributions

S.I. and M.B. conceived and co-designed the study. S.I. synthesized the mRNAs, purified the mRNAs and proteins for microinjection, examined the phenotype of TRIM21-mediated COPS3-depleted embryos (immunostainings, immunoblots), draw the figures, and analyzed the results together with M.B. M.B. performed the microinjections and embryo culture, analyzed the results including the statistical analysis, and wrote the manuscript with input from S.I. and G.F.. H.D. performed the mass spectrometry analysis. All authors approved the manuscript.

Acknowledgements

We thank the Max Planck Institute for Molecular Biomedicine and its Director, Prof. Hans R. Schöler, for infrastructural support. As part of it, we experienced outstanding support from the mouse housing facility, ensuring a dependable supply of mice needed to collect oocytes and embryos. We thank Janine Kretschmer for technical help with the COPS3 depletion, and Annalen Nolte and Lina Lüken for technical help with the LC-MS/MS measurements. We are grateful to Daniel Palmer for assistance in drawing the TreeMap in Figure 4. The Affymetrix analysis was outsourced to the Core Genomic Facility of the Faculty of Medicine of the University of Muenster (Anika Witten, Andreas Huge). Critical reading by Ivan Bedzhov of an earlier version of this manuscript is gratefully acknowledged.

References

1 Morris, S. A., Guo, Y. & Zernicka-Goetz, M. Developmental plasticity is bound by pluripotency and the Fgf and Wnt signaling pathways. *Cell Rep* **2**, 756-765, doi:10.1016/j.celrep.2012.08.029 (2012).

2 Lorthongpanich, C., Yang, S. H., Piotrowska-Nitsche, K., Parnpai, R. & Chan, A. W. Development of single mouse blastomeres into blastocysts, outgrowths and the establishment of embryonic stem cells. *Reproduction* **135**, 805-813, doi:10.1530/REP-07-0478 (2008).

3 Cui, W. *et al.* Towards Functional Annotation of the Preimplantation Transcriptome: An RNAi Screen in Mammalian Embryos. *Sci Rep* **6**, 37396, doi:10.1038/srep37396 (2016).

4 Kafer, G. R. & Cesare, A. J. A Survey of Essential Genome Stability Genes Reveals That Replication Stress Mitigation Is Critical for Peri-Implantation Embryogenesis. *Front Cell Dev Biol* **8**, 416, doi:10.3389/fcell.2020.00416 (2020).

5 Casser, E. *et al.* Differences in blastomere totipotency in 2-cell mouse embryos are a maternal trait mediated by asymmetric mRNA distribution. *Mol Hum Reprod* **25**, 729-744, doi:10.1093/molehr/gaz051 (2019).

6 Yan, J. *et al.* COP9 signalosome subunit 3 is essential for maintenance of cell proliferation in the mouse embryonic epiblast. *Mol Cell Biol* **23**, 6798-6808, doi:10.1128/mcb.23.19.6798-6808.2003 (2003).

7 Boiani, M., Casser, E., Fuellen, G. & Christians, E. S. Totipotency continuity from zygote to early blastomeres: a model under revision. *Reproduction* **158**, R49-R65, doi:10.1530/REP-18-0462 (2019).

8 Peth, A., Berndt, C., Henke, W. & Dubiel, W. Downregulation of COP9 signalosome subunits differentially affects the CSN complex and target protein stability. *BMC Biochem* **8**, 27, doi:10.1186/1471-2091-8-27 (2007).

9 Seeger, M. *et al.* A novel protein complex involved in signal transduction possessing similarities to 26S proteasome subunits. *FASEB J* **12**, 469-478 (1998).

10 Deng, X. W. *et al.* Unified nomenclature for the COP9 signalosome and its subunits: an essential regulator of development. *Trends Genet* **16**, 202-203, doi:10.1016/s0168-9525(00)01982-x (2000).

11 Wei, N. *et al.* The COP9 complex is conserved between plants and mammals and is related to the 26S proteasome regulatory complex. *Curr Biol* **8**, 919-922, doi:10.1016/s0960-9822(07)00372-7 (1998).

12 Chamovitz, D. A. Revisiting the COP9 signalosome as a transcriptional regulator. *EMBO Rep* **10**, 352-358, doi:10.1038/embor.2009.33 (2009).

13 Barth, E., Hubler, R., Baniahmad, A. & Marz, M. The Evolution of COP9 Signalosome in Unicellular and Multicellular Organisms. *Genome Biol Evol* **8**, 1279-1289, doi:10.1093/gbe/evw073 (2016).

14 Meir, M. *et al.* The COP9 signalosome is vital for timely repair of DNA double-strand breaks. *Nucleic Acids Res* **43**, 4517-4530, doi:10.1093/nar/gkv270 (2015).

15 Huang, Q. *et al.* COP9 signalosome complex subunit 5, an IFT20 binding partner, is essential to maintain male germ cell survival and acrosome biogenesis. *Biol Reprod* **102**, 233-247, doi:10.1093/biolre/ioz154 (2020).

16 Pan, L. *et al.* Protein competition switches the function of COP9 from self-renewal to differentiation. *Nature* **514**, 233-236, doi:10.1038/nature13562 (2014).

17 Kim, E. *et al.* Function of COP9 signalosome in regulation of mouse oocytes meiosis by regulating MPF activity and securing degradation. *PLoS One* **6**, e25870, doi:10.1371/journal.pone.0025870 (2011).

18 Casser, E., Israel, S., Schlatt, S., Nordhoff, V. & Boiani, M. Retrospective analysis: reproducibility of interblastomere differences of mRNA expression in 2-cell stage mouse embryos is remarkably poor due to combinatorial mechanisms of blastomere diversification. *Mol Hum Reprod* **24**, 388-400, doi:10.1093/molehr/gay021 (2018).

19 Casser, E. *et al.* Totipotency segregates between the sister blastomeres of two-cell stage mouse embryos. *Sci Rep* **7**, 8299, doi:10.1038/s41598-017-08266-6 (2017).

20 Emerson, J. A. Disruption of the cytokeratin filament network in the preimplantation mouse embryo. *Development* **104**, 219-234 (1988).

21 Clift, D. *et al.* A Method for the Acute and Rapid Degradation of Endogenous Proteins. *Cell* **171**, 1692-1706 e1618, doi:10.1016/j.cell.2017.10.033 (2017).

22 Israel, S., Casser, E., Drexler, H. C. A., Fuellen, G. & Boiani, M. A framework for TRIM21-mediated protein depletion in early mouse embryos: recapitulation of Tead4 null phenotype over three days. *BMC Genomics* **20**, 755, doi:10.1186/s12864-019-6106-2 (2019).

23 Geiger, T., Wehner, A., Schaab, C., Cox, J. & Mann, M. Comparative proteomic analysis of eleven common cell lines reveals ubiquitous but varying expression of most proteins. *Mol Cell Proteomics* **11**, M111 014050, doi:10.1074/mcp.M111.014050 (2012).

24 Schwanhausser, B. *et al.* Global quantification of mammalian gene expression control. *Nature* **473**, 337-342, doi:10.1038/nature10098 (2011).

25 Shin, J. B. *et al.* Molecular architecture of the chick vestibular hair bundle. *Nat Neurosci* **16**, 365-374, doi:10.1038/nn.3312 (2013).
26 Israel, S. *et al.* An integrated genome-wide multi-omics analysis of gene expression dynamics in the preimplantation mouse embryo. *Sci Rep* **9**, 13356, doi:10.1038/s41598-019-49817-3 (2019).
27 Mehlmann, L. M., Uliasz, T. F. & Lowther, K. M. SNAP23 is required for constitutive and regulated exocytosis in mouse oocytes. *Biol Reprod* **101**, 338-346, doi:10.1093/biolre/ioz106 (2019).
28 Yu, J., Hecht, N. B. & Schultz, R. M. Expression of MSY2 in mouse oocytes and preimplantation embryos. *Biol Reprod* **65**, 1260-1270 (2001).
29 Qin, D. *et al.* The subcortical maternal complex protein Nlrp4f is involved in cytoplasmic lattice formation and organelle distribution. *Development* **146**, doi:10.1242/dev.183616 (2019).
30 Gallicano, G. I., Larabell, C. A., McGaughey, R. W. & Capco, D. G. Novel cytoskeletal elements in mammalian eggs are composed of a unique arrangement of intermediate filaments. *Mech Dev* **45**, 211-226, doi:10.1016/0925-4773(94)90009-4 (1994).
31 Supek, F., Bosnjak, M., Skunca, N. & Smuc, T. REVIGO summarizes and visualizes long lists of gene ontology terms. *PLoS One* **6**, e21800, doi:10.1371/journal.pone.0021800 (2011).
32 Svoboda, P., Franke, V. & Schultz, R. M. Sculpting the Transcriptome During the Oocyte-to-Embryo Transition in Mouse. *Curr Top Dev Biol* **113**, 305-349, doi:10.1016/bs.ctdb.2015.06.004 (2015).
33 Abe, K. I. *et al.* Minor zygotic gene activation is essential for mouse preimplantation development. *Proc Natl Acad Sci U S A* **115**, E6780-E6788, doi:10.1073/pnas.1804309115 (2018).
34 Mamo, S., Gal, A. B., Bodo, S. & Dinnyes, A. Quantitative evaluation and selection of reference genes in mouse oocytes and embryos cultured in vivo and in vitro. *BMC Dev Biol* **7**, 14, doi:10.1186/1471-213X-7-14 (2007).
35 Liu, Y., Zhao, L. W., Shen, J. L., Fan, H. Y. & Jin, Y. Maternal DCAF13 Regulates Chromatin Tightness to Contribute to Embryonic Development. *Sci Rep* **9**, 6278, doi:10.1038/s41598-019-42179-w (2019).
36 Parisi, T. *et al.* Cyclins E1 and E2 are required for endoreplication in placental trophoblast giant cells. *EMBO J* **22**, 4794-4803, doi:10.1093/emboj/cdg482 (2003).
37 Lykke-Andersen, K. *et al.* Disruption of the COP9 signalosome Csn2 subunit in mice causes deficient cell proliferation, accumulation of p53 and cyclin E, and early embryonic death. *Mol Cell Biol* **23**, 6790-6797, doi:10.1128/mcb.23.19.6790-6797.2003 (2003).
38 Menon, S. *et al.* COP9 signalosome subunit 8 is essential for peripheral T cell homeostasis and antigen receptor-induced entry into the cell cycle from quiescence. *Nat Immunol* **8**, 1236-1245, doi:10.1038/ni1514 (2007).
39 Tomoda, K., Yoneda-Kato, N., Fukumoto, A., Yamanaka, S. & Kato, J. Y. Multiple functions of Jab1 are required for early embryonic development and growth potential in mice. *J Biol Chem* **279**, 43013-43018, doi:10.1074/jbc.M406559200 (2004).
40 Zhao, R. *et al.* Subunit 6 of the COP9 signalosome promotes tumorigenesis in mice through stabilization of MDM2 and is upregulated in human cancers. *J Clin Invest* **121**, 851-865, doi:10.1172/JCI44111 (2011).
41 Bebbere, D., Masala, L., Albertini, D. F. & Ledda, S. The subcortical maternal complex: multiple functions for one biological structure? *J Assist Reprod Genet* **33**, 1431-1438, doi:10.1007/s10815-016-0788-z (2016).
42 Li, L., Baibakov, B. & Dean, J. A subcortical maternal complex essential for preimplantation mouse embryogenesis. *Dev Cell* **15**, 416-425, doi:10.1016/j.devcel.2008.07.010 (2008).
43 Tong, Z. B. *et al.* Mater, a maternal effect gene required for early embryonic development in mice. *Nat Genet* **26**, 267-268, doi:10.1038/81547 (2000).
44 Wu, X. *et al.* Zygote arrest 1 (Zar1) is a novel maternal-effect gene critical for the oocyte-to-embryo transition. *Nat Genet* **33**, 187-191, doi:10.1038/ng1079 (2003).
45 Christians, E., Davis, A. A., Thomas, S. D. & Benjamin, I. J. Maternal effect of Hsf1 on reproductive success. *Nature* **407**, 693-694, doi:10.1038/35037669 (2000).
46 Bultman, S. J. *et al.* Maternal BRG1 regulates zygotic genome activation in the mouse. *Genes Dev* **20**, 1744-1754, doi:10.1101/gad.1435106 (2006).
47 Condic, M. L. The Role of Maternal-Effect Genes in Mammalian Development: Are Mammalian Embryos Really an Exception? *Stem Cell Rev* **12**, 276-284, doi:10.1007/s12015-016-9648-6 (2016).
48 Chen, V. C., Kristensen, A. R., Foster, L. J. & Naus, C. C. Association of connexin43 with E3 ubiquitin ligase TRIM21 reveals a mechanism for gap junction phosphodegron control. *J Proteome Res* **11**, 6134-6146, doi:10.1021/pr300790h (2012).
49 Guha, A., Nag, S. & Ray, P. S. Negative feedback regulation by HuR controls TRIM21 expression and function in response to UV radiation. *Sci Rep* **10**, 11753, doi:10.1038/s41598-020-68646-3 (2020).
50 Xie, S. *et al.* HDAC6 regulates antibody-dependent intracellular neutralization of viruses via deacetylation of TRIM21. *J Biol Chem* **295**, 14343-14351, doi:10.1074/jbc.RA119.011006 (2020).

51 Glickman, M. H. *et al.* A subcomplex of the proteasome regulatory particle required for ubiquitin-conjugate degradation and related to the COP9-signalosome and eIF3. *Cell* **94**, 615-623, doi:10.1016/s0092-8674(00)81603-7 (1998).
52 Scheel, H. & Hofmann, K. Prediction of a common structural scaffold for proteasome lid, COP9-signalosome and eIF3 complexes. *BMC Bioinformatics* **6**, 71, doi:10.1186/1471-2105-6-71 (2005).
53 Pfeiffer, M. J. *et al.* Reprogramming of two somatic nuclei in the same ooplasm leads to pluripotent embryonic stem cells. *Stem Cells* **31**, 2343-2353, doi:10.1002/stem.1497 (2013).
54 Mu, X. F., Jin, X. L., Farnham, M. M., Li, Y. & O'Neill, C. DNA damage-sensing kinases mediate the mouse 2-cell embryo's response to genotoxic stress. *Biol Reprod* **85**, 524-535, doi:10.1095/biolreprod.110.089334 (2011).
55 Wang, Y. *et al.* Deletion of the Cul1 gene in mice causes arrest in early embryogenesis and accumulation of cyclin E. *Curr Biol* **9**, 1191-1194, doi:10.1016/S0960-9822(00)80024-X (1999).
56 Xu, Y. W. *et al.* Maternal DCAF2 is crucial for maintenance of genome stability during the first cell cycle in mice. *J Cell Sci* **130**, 3297-3307, doi:10.1242/jcs.206664 (2017).
57 Dealy, M. J. *et al.* Loss of Cul1 results in early embryonic lethality and dysregulation of cyclin E. *Nat Genet* **23**, 245-248, doi:10.1038/13886 (1999).
58 Liu, C. L., Yu, I. S., Pan, H. W., Lin, S. W. & Hsu, H. C. L2dtl is essential for cell survival and nuclear division in early mouse embryonic development. *J Biol Chem* **282**, 1109-1118, doi:10.1074/jbc.M606535200 (2007).
59 Hu, K. On Mammalian Totipotency: What Is the Molecular Underpinning for the Totipotency of Zygote? *Stem Cells Dev* **28**, 897-906, doi:10.1089/scd.2019.0057 (2019).
60 Zalzman, M. *et al.* Zscan4 regulates telomere elongation and genomic stability in ES cells. *Nature* **464**, 858-863, doi:10.1038/nature08882 (2010).
61 Kim, B., Kan, R., Anguish, L., Nelson, L. M. & Coonrod, S. A. Potential role for MATER in cytoplasmic lattice formation in murine oocytes. *PLoS One* **5**, e12587, doi:10.1371/journal.pone.0012587 (2010).
62 van der Ploeg, R. R., Böhm, W. & Kirkham, M. B. On the origin of the theory of mineral nutrition of plants and the law of the minimum. *Soil Sci. Soc. Am. J.* **63**, 1055–1062 (1999).
63 El-Brolosy, M. A. & Stainier, D. Y. R. Genetic compensation: A phenomenon in search of mechanisms. *PLoS Genet* **13**, e1006780, doi:10.1371/journal.pgen.1006780 (2017).
64 Smith, I. *et al.* Evaluation of RNAi and CRISPR technologies by large-scale gene expression profiling in the Connectivity Map. *PLoS Biol* **15**, e2003213, doi:10.1371/journal.pbio.2003213 (2017).
65 Chi, F., Sharpley, M. S., Nagaraj, R., Roy, S. S. & Banerjee, U. Glycolysis-Independent Glucose Metabolism Distinguishes TE from ICM Fate during Mammalian Embryogenesis. *Dev Cell* **53**, 9-26 e24, doi:10.1016/j.devcel.2020.02.015 (2020).
66 Drutovic, D., Duan, X., Li, R., Kalab, P. & Solc, P. RanGTP and importin beta regulate meiosis I spindle assembly and function in mouse oocytes. *EMBO J* **39**, e101689, doi:10.15252/embj.2019101689 (2020).
67 Firmani, L. *The G Protein-Coupled Receptor, GPR3, Promotes the Acquisition of Oocyte Meiotic Competence* Doctor of Philosophy thesis, University of Connecticut, (2018).
68 Sha, Q. Q. *et al.* Characterization of zygotic genome activation-dependent maternal mRNA clearance in mouse. *Nucleic Acids Res* **48**, 879-894, doi:10.1093/nar/gkz1111 (2020).
69 So, C. *et al.* A liquid-like spindle domain promotes acentrosomal spindle assembly in mammalian oocytes. *Science* **364**, doi:10.1126/science.aat9557 (2019).
70 Wang, H. *et al.* Symmetry breaking in hydrodynamic forces drives meiotic spindle rotation in mammalian oocytes. *Sci Adv* **6**, eaaz5004, doi:10.1126/sciadv.aaz5004 (2020).
71 Zhou, C. J. *et al.* Loss of CENPF leads to developmental failure in mouse embryos. *Cell Cycle* **18**, 2784-2799, doi:10.1080/15384101.2019.1661173 (2019).
72 Zielinska, A. P. *et al.* Meiotic Kinetochores Fragment into Multiple Lobes upon Cohesin Loss in Aging Eggs. *Curr Biol* **29**, 3749-3765 e3747, doi:10.1016/j.cub.2019.09.006 (2019).
73 Gerri, C. *et al.* Initiation of a conserved trophectoderm program in human, cow and mouse embryos. *Nature* **587**, 443-447, doi:10.1038/s41586-020-2759-x (2020).
74 Eisa, A. A. *et al.* X-Linked Huwe1 Is Essential for Oocyte Maturation and Preimplantation Embryo Development. *iScience* **23**, 101523, doi:10.1016/j.isci.2020.101523 (2020).
75 Avilion, A. A. *et al.* Multipotent cell lineages in early mouse development depend on SOX2 function. *Genes Dev* **17**, 126-140, doi:10.1101/gad.224503 (2003).
76 Shen-Li, H. *et al.* Essential role for Max in early embryonic growth and development. *Genes Dev* **14**, 17-22 (2000).
77 Nagaraj, R. *et al.* Nuclear Localization of Mitochondrial TCA Cycle Enzymes as a Critical Step in Mammalian Zygotic Genome Activation. *Cell* **168**, 210-223 e211, doi:10.1016/j.cell.2016.12.026 (2017).
78 Percie du Sert, N. *et al.* The ARRIVE guidelines 2.0: Updated guidelines for reporting animal research. *PLoS Biol* **18**, e3000410, doi:10.1371/journal.pbio.3000410 (2020).

79 Ho, Y., Wigglesworth, K., Eppig, J. J. & Schultz, R. M. Preimplantation development of mouse embryos in KSOM: augmentation by amino acids and analysis of gene expression. *Mol Reprod Dev* **41**, 232-238, doi:10.1002/mrd.1080410214 (1995).
80 Heberle, H., Meirelles, G. V., da Silva, F. R., Telles, G. P. & Minghim, R. InteractiVenn: a web-based tool for the analysis of sets through Venn diagrams. *BMC Bioinformatics* **16**, 169, doi:10.1186/s12859-015-0611-3 (2015).
81 Schwarzer, C. *et al.* ART culture conditions change the probability of mouse embryo gestation through defined cellular and molecular responses. *Hum Reprod* **27**, 2627-2640, doi:10.1093/humrep/des223 (2012).
82 Wang, Q. & Latham, K. E. Requirement for protein synthesis during embryonic genome activation in mice. *Mol Reprod Dev* **47**, 265-270, doi:10.1002/(SICI)1098-2795(199707)47:3<265::AID-MRD5>3.0.CO;2-J (1997).
83 Shin, S. W. *et al.* Inhibition of the ubiquitin-proteasome system leads to delay of the onset of ZGA gene expression. *J Reprod Dev* **56**, 655-663, doi:10.1262/jrd.10-104m (2010).
84 Antczak, M. & Van Blerkom, J. Oocyte influences on early development: the regulatory proteins leptin and STAT3 are polarized in mouse and human oocytes and differentially distributed within the cells of the preimplantation stage embryo. *Mol Hum Reprod* **3**, 1067-1086, doi:10.1093/molehr/3.12.1067 (1997).
85 Antczak, M. & Van Blerkom, J. Temporal and spatial aspects of fragmentation in early human embryos: possible effects on developmental competence and association with the differential elimination of regulatory proteins from polarized domains. *Hum Reprod* **14**, 429-447, doi:10.1093/humrep/14.2.429 (1999).
86 Schulz, L. C. & Roberts, R. M. Dynamic changes in leptin distribution in the progression from ovum to blastocyst of the pre-implantation mouse embryo. *Reproduction* **141**, 767-777, doi:10.1530/REP-10-0532 (2011).
87 Cavaleri, F., Gentile, L., Scholer, H. R. & Boiani, M. Recombinant human albumin supports development of somatic cell nuclear transfer embryos in mice: toward the establishment of a chemically defined cloning protocol. *Cloning Stem Cells* **8**, 24-40, doi:10.1089/clo.2006.8.24 (2006).
88 Vizcaino, J. A. *et al.* The PRoteomics IDEntifications (PRIDE) database and associated tools: status in 2013. *Nucleic Acids Res* **41**, D1063-1069, doi:10.1093/nar/gks1262 (2013).
89 Perez-Riverol, Y. *et al.* The PRIDE database and related tools and resources in 2019: improving support for quantification data. *Nucleic Acids Res* **47**, D442-D450, doi:10.1093/nar/gky1106 (2019).

Figures

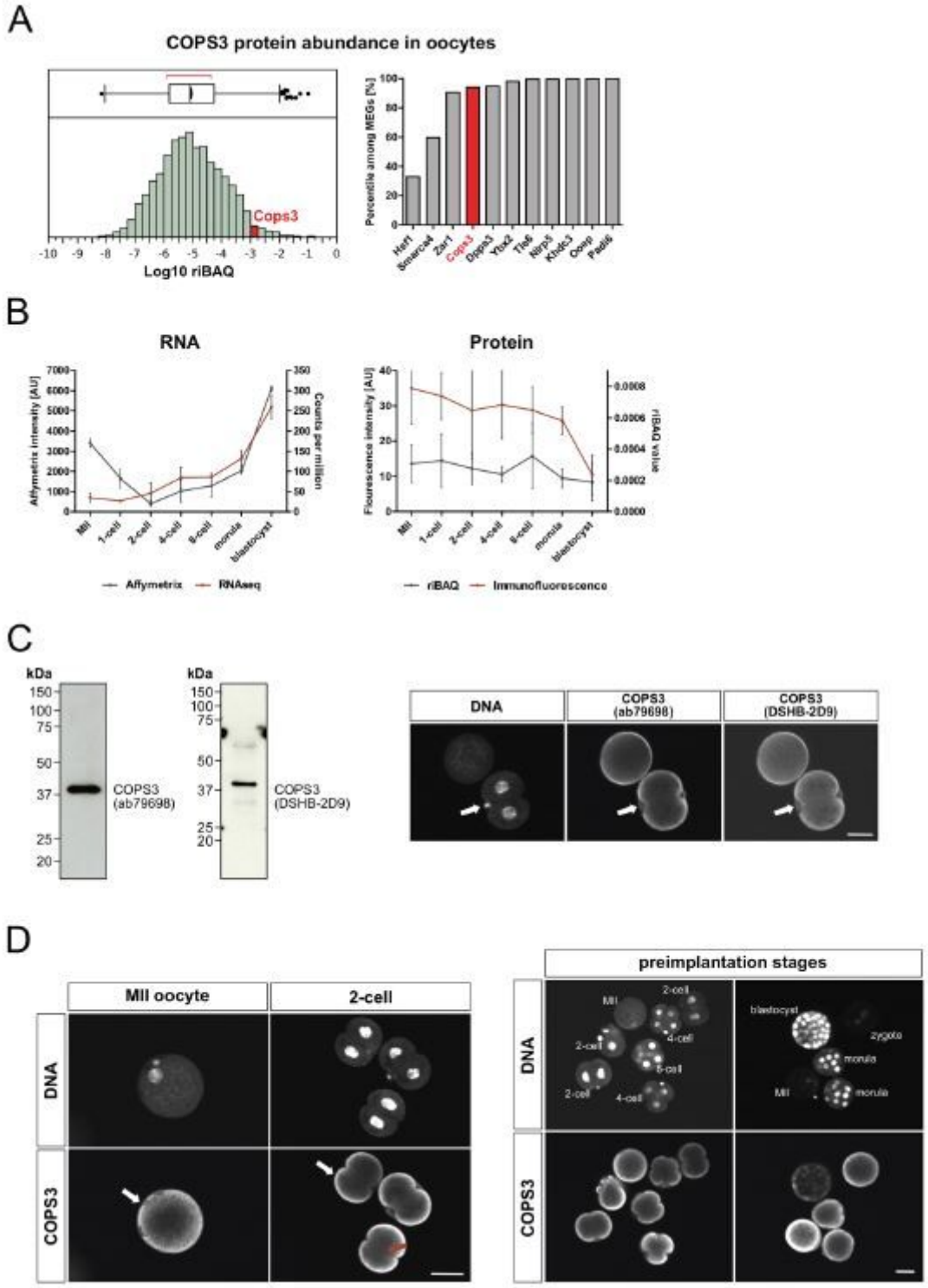

Figure 1

Protein and transcript expression of Cops3 in mouse preimplantation development. (A). Left: Genome-wide distribution of protein abundances (riBAQ) in oocytes. Right: Compared to maternal factors known to be accumulated in oocytes, the abundance of COPS3 ranks high in the 94th percentile. (B). Abundance

profile of Cops3 mRNA and COPS3 protein, each measured by two independent methods; data are presented as means and standard deviations (for RNA, 100 oocytes or embryos per stage in two replicates; for protein, 200-600 oocytes or embryos per stage in three proteomic replicates, and at least 3 oocytes or embryos per stage for immunofluorescence; transcriptome/proteome datasets are extracted from 26 and are provided here in Supplementary Tables 1 and 2). (C). Specificity of the two monoclonal antibodies against COPS3 used in this study, RabMab® (ab79698) and mouse (DSHB- 2D9), as documented by the single band in Western blot (lysate of MEFs or ES cells) and by the subcellular distribution within the same 2-cell embryos after immunofluorescence with both antibodies. The full-length blots are presented in Supplementary Figure 1. White arrow points at the non-stained polar body next to the positive rim. Note the lower background, i.e. the better signal-to-noise ratio, of the RabMab®. DNA was stained with YO-PRO-1. (D). Left: Developmental localization of COPS3 in oocyte and 2-cell stage, visualized by the RabMab® antibody, with white arrows pointing at the cortical rim and red arrow pointing at the signal exclusion from regions of cell-cell contact. Right: Developmental localization of COPS3 in preimplantation stages; note the prominence of the cortical rim up to the 4-cell stage, starting to fade thereafter, and being replaced by a nuclear signal distribution at the blastocyst stage. DNA was stained with YO-PRO-1. Abbreviations: Affymetrix stands for microarray; AU, arbitrary units; ES cells, embryonic stem cells; MEFs, mouse embryonic fibroblasts; MEG, maternal-effect genes; kDa, kiloDalton. riBAQ, relative intensity-based absolute quantification. Size bar: 50 μm.

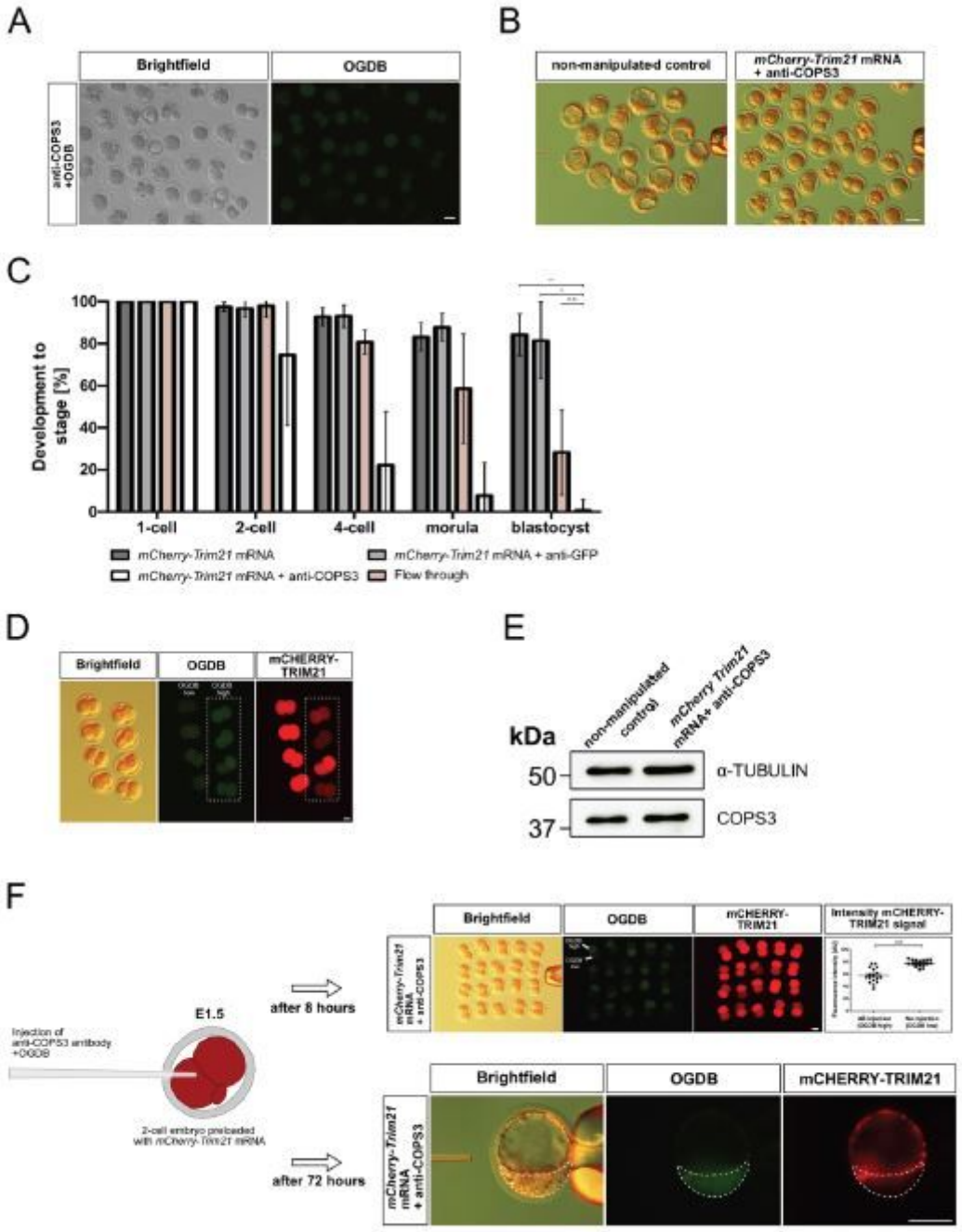

Figure 2

COPS3 is required for embryonic progression past the 2-cell stage in mice. (A). Representative brightfield images of zygotes (N = 48) which arrested after one cleavage when microinjected with anti-COPS3 antibody and OGDB, and formed no blastocysts (96 % blastocysts in control group, N = 28). Note that inert OGDB but not mCherry- Trim21 mRNA was co-injected. (B). Representative images of zygotes (N = 285) which arrested after one cleavage when microinjected with mCherry-Trim21 mRNA, anti-COPS3 antibody and OGDB, in contrast to the blastocyst progression of non-manipulated controls. (C). Developmental rates of zygotes microinjected with mCherry-Trim21 mRNA (N = 212), mCherry-Trim21 mRNA + anti-COPS3 antibody (N = 285), mCherry-Trim21 mRNA + anti-GFP antibody (N = 245) or the

buffer of anti-COPS3 antibody (1st flow of the antibody through the purification column, N = 99); data are presented as means and standard deviations, P values are calculated by t-test. (D). mCHERRY-COPS3 fluorescence intensity was reduced but not completely abolished by the TRIM21 reaction, as visualized in eight embryos, all of which were preloaded with mCherry-Trim21 mRNA at the 1-cell stage, but only the four embryos to the right also received COPS3 antibody 6 h after the mRNA (embryos in dotted box). Note that inert OGDB was co-injected, so as to identify a posteriori which embryos received only mRNA (OGDB low) and which embryos additionally received the antibody (OGDB high). (E). Western blot analysis (200 2-cell embryos) reveals that the total amount of COPS3 is not affected by TRIM21-mediated proteasomal degradation. The full-length blot is presented in Supplementary Figure 1. (F). Side-by-side comparison of the sister blastomeres, both preloaded with mCherry-Trim21 mRNA but only one receiving also the antibody (N = 20). The kinetics of the proteasomal degradation of COPS3 is slow, as visualized by mCHERRY fluorescence after 8 hours, which is completely abolished only after 72 hours. The blastomere fails to cleave further (dotted line). **, $P < 0.01$. Abbreviations: OGDB, Oregon-green dextran beads; n.s., not significant. Size bar: 50 μm.

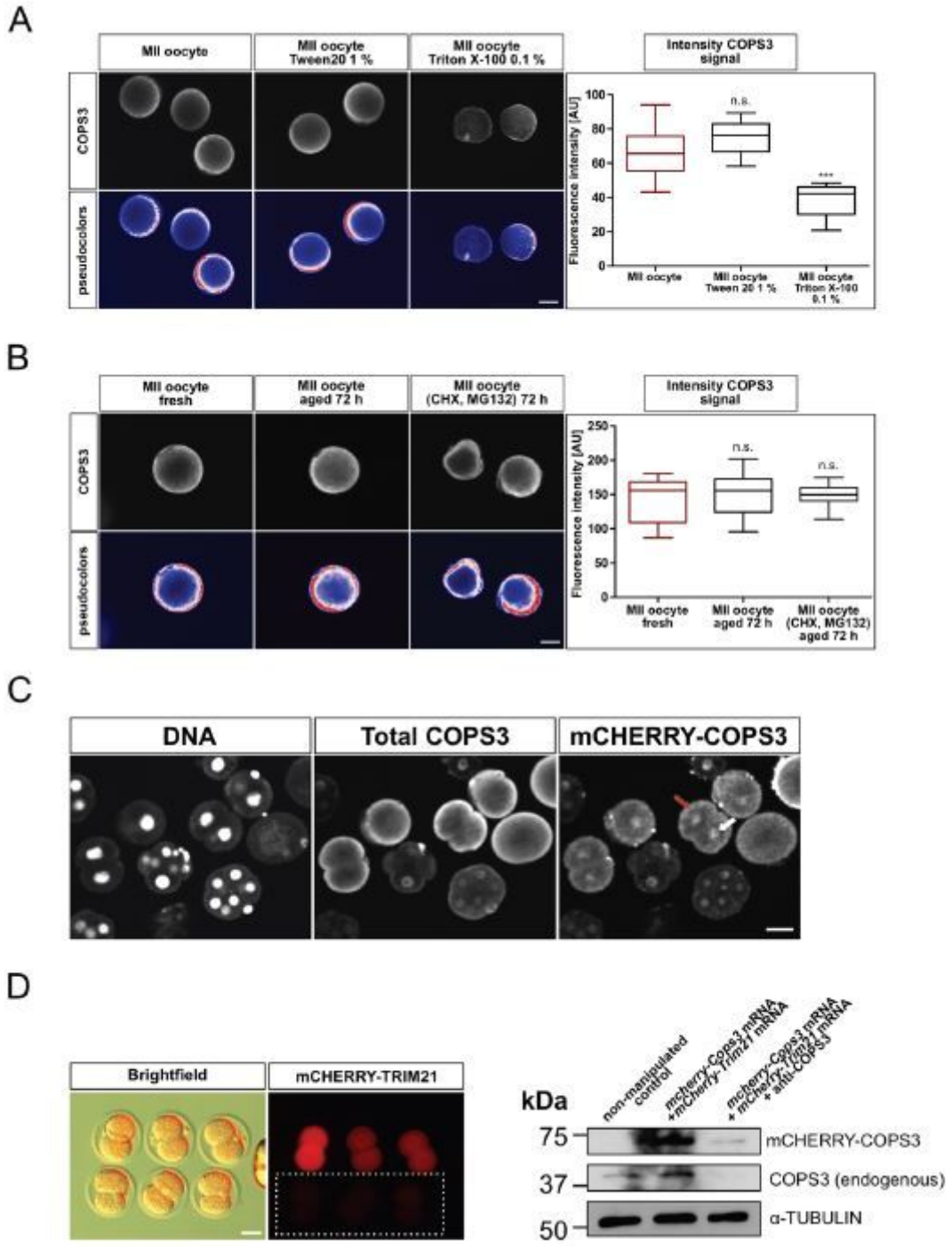

Figure 3

The cortical rim of COPS3 is refractory to spontaneous degradation and chemical extraction. (A). COPS3 is completely refractory to chemical extraction using Tween 20, and residues of COPS3 are seen also after extraction with Triton X-100. Compared to untreated oocytes, the cortical rim of COPS3 is still present, albeit thinned, in live oocytes extracted for 10 min with 1 % Tween 20 or 0.1 % Triton X-100 (N = 11, 11, 13, respectively). (B). COPS3 is refractory to spontaneous degradation, such as that taking place during oocyte aging in vitro in the presence of inhibitors of protein synthesis (CHX) and protein degradation (MG132) (MII fresh, n = 48; MII aged 72 h, n = 10; MII treated with CHX and MG132, n = 10).

Representative images are shown, either raw or pseudocolored in Fiji using the LUT 'Union jack.' Data in the box plots are presented as median, 1st and 3rd quartiles, and range (whiskers). P values are calculated by the Wilcoxon test, setting the MII oocyte as the reference (painted red in the plot). ***, P < 0.001. (C). Immunofluorescent co-staining of endogenous and exogenous COPS3 after overexpression of mCherry-Cops3 mRNA. Images show that the exogenous COPS3 is mostly taken up in the nucleus (white arrow) but it also gains access to the cortical rim (red arrow). DNA was stained with YO-PRO-1. (D). After overexpression of COPS3, the 'Trim-away' reaction attains effectiveness as revealed by loss of mCHERRY fluorescence in live-cell imaging (dotted box) and depletion of mCHERRY-COPS3 in Western blot. The full-length blot is presented in Supplementary Figure 1. Abbreviations: CHX, cycloheximide; MG132, proteasome inhibitor; n.s., not significant. Size bar: 50 μm.

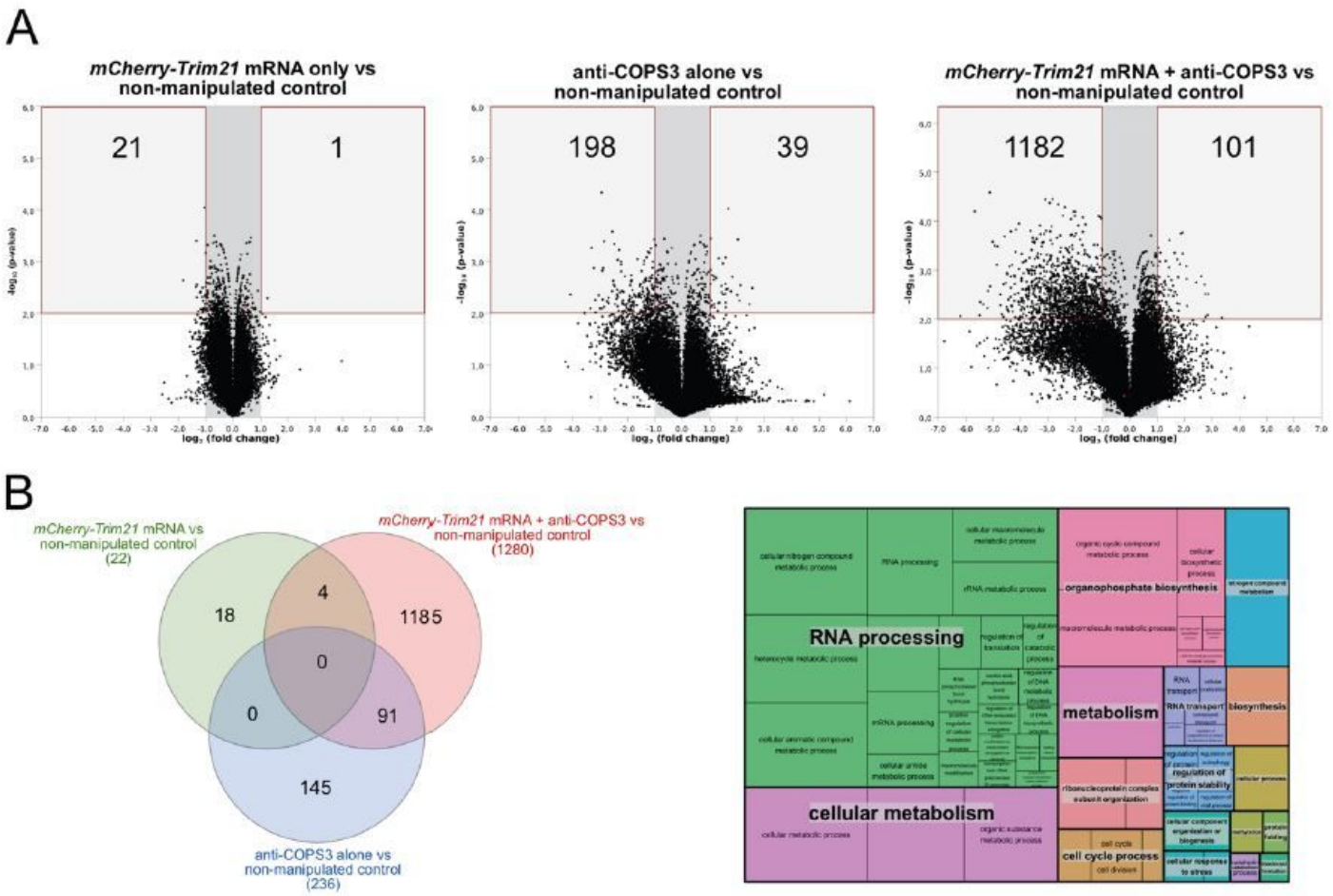

Figure 4

TRIM21-mediated COPS3 inactivation but not TRIM21 brings about a large perturbation of gene expression at the 2-cell stage. (A). Volcano plots show the effect of TRIM21 (left), COPS3 antibody (center) and TRIM21+antibody (right) on the embryo transcriptome at the 2-cell stage. The data point of Cops3 mRNA is painted red. The numbers of mRNAs that are under- vs. over-expressed (fold change ≥ 2, p ≤ 0.01, t-test.) are shown in the upper corners. (B). (Left) Venn diagram recapitulating the number of transcripts that are differently expressed in either direction – up or down (fold change ≥ 2, p ≤ 0.01, t-test)

as a result of the same treatments that were compared pairwise in the volcano plots. (Right) TreeMap view of the 1421 mRNAs identified by the Venn diagram. Each rectangle is a single cluster representative. The representatives are joined into ‘superclusters’ of loosely related terms, visualized with different colors. The size of the rectangles was adjusted to reflect the number of the gene ontology terms in the cluster representative.

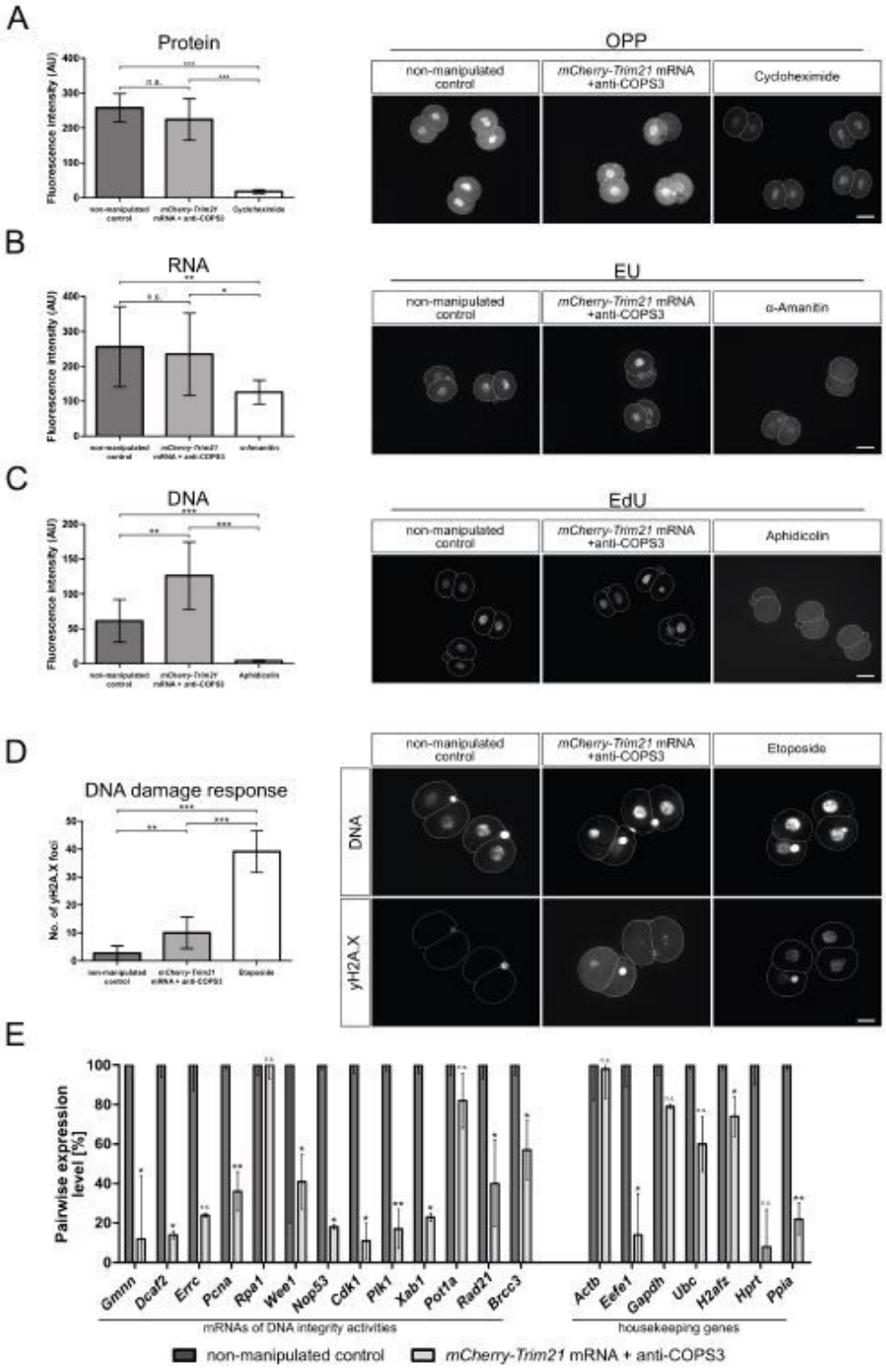

Figure 5

DNA is affected by antibody-mediated COPS3 inactivation but not RNA or protein synthesis. (A). Histogram (left) and representative pictures (right) show that COPS3-inactivated zygotes incorporated the OPP precursor for protein synthesis to the same extent as non-manipulated controls, while the protein synthesis inhibitor cycloheximide reduced the incorporation (N = 12, 14, 11, respectively). (B). COPS3-inactivated zygotes incorporated the EU precursor for RNA synthesis to the same extent as non-manipulated controls, while the RNA polymerase II inhibitor α-amanitin reduced the incorporation (N = 5, 6, 4, respectively). (C). COPS3-inactivated zygotes incorporated the EdU precursor for DNA synthesis to a higher extent than non-manipulated controls, while the DNA polymerase inhibitor aphidicolin reduced the incorporation (N = 5, 7, 11, respectively). (D). COPS3-inactivated zygotes presented more histone γH2A.X foci per nucleus than non-manipulated controls, while the topoisomerase inhibitor etoposide increased the number of foci even more (N = 11, 11, 8, respectively). (E). Transcript levels of key genes involved in the prevention of DNA endoreduplication and actuation of DNA double-strand break repair as well as housekeeping genes (from transcriptome data, dataset GSE155205; Supplementary Table 2). Data are presented as means and standard deviations. P values are calculated by t-test. *, P < 0.05. **, P < 0.01. ***, P < 0.001. Abbreviations: wt, wildtype; OPP, O-propargyl-puromycin; EU, 5-ethynyl uridine; EdU, 5-ethynyl-2'-deoxyuridine; ns, not significant. Size bar: 50 μm.

Supplementary Files

This is a list of supplementary files associated with this preprint. Click to download.

- SupplementaryTable1Israeletal.xlsx
- SupplementaryTable2Israeletal.xlsx
- SupplementaryfiguresIsraeletal.pdf